Atmos. Chem. Phys. Discuss., https://doi.org/10.5194/acp-2017-1109
Manuscript under review for journal Atmos. Chem. Phys.
Discussion started: 2 January 2018

Atmospheric Chemistry and Physics Discussions

Large Contributions from Biogenic Monoterpenes and Sesquiterpenes to Organic Aerosol in the Southeastern United States

Lu Xu[1,a], Havala O.T. Pye[2], Jia He[3], Yunle Chen[4], Benjamin N. Murphy[2], Nga Lee Ng[1,3*]

[1]School of Chemical and Biomolecular Engineering, Georgia Institute of Technology, Atlanta, GA 30332, USA

[2]National Exposure Research Laboratory, US Environmental Protection Agency, Research Triangle Park, NC 27711, USA

[3]School of Earth and Atmospheric Sciences, Georgia Institute of Technology, Atlanta, GA 30332, USA

[4]School of Materials Science and Engineering, Georgia Institute of Technology, Atlanta, GA 30332, USA

[*]To whom correspondence should be addressed. E-mail: ng@chbe.gatech.edu

[a]Present address: Division of Geological and Planetary Sciences, California Institute of Technology, Pasadena, CA 91125, USA

Atmos. Chem. Phys. Discuss., https://doi.org/10.5194/acp-2017-1109
Manuscript under review for journal Atmos. Chem. Phys.
Discussion started: 2 January 2018

Atmospheric Chemistry and Physics Discussions

Abstract

Atmospheric organic aerosol (OA) has important impacts on climate and human health but its sources remain poorly understood. Biogenic monoterpenes and sesquiterpenes are critical precursors of OA. The OA generation from these precursors predicted by models has considerable uncertainty owing to a lack of appropriate observations as constraints. Here, we perform novel lab-in-the-field experiments, which allow us to study OA formation under realistic atmospheric conditions and offer a connection between laboratory and field studies. Based on the lab-in-the-field experimental approach and positive matrix factorization analysis on aerosol mass spectrometry data, we provide a measure of OA from monoterpenes and sesquiterpenes in the southeastern U.S. Further, we use an upgraded atmospheric model and reproduce the measured OA concentration from monoterpenes and sesquiterpenes at multiple sites in the southeastern U.S., building confidence in the observed attribution of monoterpene SOA. We show that the annual average concentration of OA from monoterpenes and sesquiterpenes in the southeastern U.S. is ~2.1 μg m^{-3}. This amount is substantially higher than represented in current regional models and accounts for 21% of World Health Organization $PM_{2.5}$ standard, indicating a significant contributor of environmental risk to the 77 million habitants in the southeastern U.S.

Atmos. Chem. Phys. Discuss., https://doi.org/10.5194/acp-2017-1109
Manuscript under review for journal Atmos. Chem. Phys.
Discussion started: 2 January 2018

1 Introduction

Organic aerosol (OA) constitutes a substantial fraction of ambient fine particulate matter (PM) and has large impacts on air quality, climate change, and human health (Carslaw et al., 2013; Lelieveld et al., 2015). OA can be directly emitted from sources (primary OA, POA) or formed by the oxidation of volatile organic compounds (VOCs) (secondary OA, SOA). Global measurements revealed the dominance of SOA over POA in various atmospheric environments (Jimenez et al., 2009; Ng et al., 2010). The VOCs can be emitted from natural sources (i.e., biogenic) or human activities (i.e., anthropogenic). However, the relative contribution of biogenic and anthropogenic sources to SOA formation in the atmosphere is poorly constrained. This knowledge is critical for formulating effective pollution control strategies that aim at reducing ambient PM concentrations and accurately assessing the climate effects of OA (Hallquist et al., 2009). Biogenic VOCs such as monoterpenes (MT, $C_{10}H_{16}$) and sesquiterpenes (SQT, $C_{15}H_{24}$) are recognized as critical precursors of SOA (Tsigaridis et al., 2014; Hodzic et al., 2016; Pye et al., 2010). The predicted global SOA production from MT and SQT varies from 14 to 246 Tg yr^{-1} (Spracklen et al., 2011; Pye et al., 2010). This large variation in model estimates arises from a number of factors (including uncertainty in SOA yield) and introduces significant uncertainties in estimating OA concentrations and its subsequent influences on climate and human exposure.

The large model uncertainties call for ambient observations to constrain model results. Isolating and measuring SOA production from specific sources are challenging because SOA is a complex mixture consisting of thousands of compounds and SOA evolves dynamically in the atmosphere. A widely used method to apportion OA into different characteristic sources is positive matrix factorization (PMF) analysis on the organic mass spectra measured by aerosol mass spectrometer (AMS) (Ulbrich et al., 2009; Jimenez et al., 2009; Ng et al., 2010). PMF-AMS analysis groups OA constituents with similar mass spectra and temporal variations into characteristic OA subtypes (i.e., factors). This analysis has revealed two ubiquitous OA subtypes in ambient environments, less-oxidized oxygenated OA (LO-OOA) and more-oxidized oxygenated OA (MO-OOA), which are differentiated by their degree of carbon oxidation. LO-OOA and MO-OOA together account for more than half of total submicron OA (Crippa et al., 2014; Xu et al., 2015a; Jimenez et al., 2009). Primarily based on comparison of their mass spectra with those of laboratory-generated SOA, previous studies proposed that LO-OOA is freshly formed SOA from various sources and evolves into MO-OOA with photochemical aging in the

atmosphere (Jimenez et al., 2009; Ng et al., 2010). These studies have significantly advanced our knowledge of the composition and evolution of ambient OA; however, there are still uncertainties associated with the sources of these OA factors. Firstly, the current understanding on LO-OOA and MO-OOA offers little mechanistic information regarding the specific sources of these factors at a measurement site. Atmospheric models typically use the lumped LO-OOA and MO-OOA concentration to constrain simulated total SOA concentration (Spracklen et al., 2011; Tsigaridis et al., 2014), which hinders our ability to diagnose the cause for the discrepancies between modeled and observed aerosol concentrations (Spracklen et al., 2011). Secondly, the assumption that LO-OOA represents fresh SOA has yet to be directly verified. Also, it is not known whether fresh SOA is exclusively apportioned into LO-OOA. For example, rather than being produced from continued photochemical aging, recent studies hypothesize that the rapidly produced HOMs (highly oxygenated molecules) from the oxidation of VOCs may contribute to MO-OOA (Ehn et al., 2014). Thus, considering the large abundance of these two OA subtypes and that they are surrogates for ambient SOA, understanding the sources of compounds composing these two OA subtypes is critical to constrain atmospheric models and SOA budget.

In this study, we integrate lab-in-the-field experiments, extensive ambient ground measurements, and state-of-the-art modeling to constrain the OA budget from MT and SQT. We provide direct evidence that newly formed SOA from α-pinene (representative monoterpene, which accounts for about half of monoterpenes emissions (Guenther et al., 2012)) and β-caryophyllene (representative sesquiterpene) dominantly contributes to LO-OOA in the southeastern U.S. The modeled SOA from the oxidation of MT and SQT (denoted as SOA_{MT+SQT}) accurately reproduces the magnitude and diurnal variability of LO-OOA measured at multiple sites in the southeastern U.S. The agreement between model and measurements supports the hypothesis that LO-OOA can be used as a measure of SOA_{MT+SQT} in the southeastern U.S. The lab-in-the-field approach allows for the study of SOA formation under realistic atmospheric conditions, which bridges laboratory studies and field measurements and provides a direct way to evaluate the atmospheric relevancy of laboratory studies.

2 Method

2.1 Lab-in-the-field perturbation experiments

The perturbation experiments were performed in July-August 2016 on the rooftop of the Environmental Science and Technology building on the Georgia Institute of Technology campus.

This measurement site is a representative urban site in Atlanta. Multiple ambient field studies have been performed at this site previously (Xu et al., 2015b; Hennigan et al., 2009; Verma et al., 2014). A 2m^3 Teflon chamber (cubic shape) (Fig. 1) was placed outdoor on the rooftop of the building. The eight corners of the chamber were open (~2"×2") to the atmosphere to allow for continuous exchange of air with the atmosphere. The perturbation procedure is briefly described below and illustrated in Fig. A1. Firstly, we continuously flushed the chamber with ambient air using two fans, which were placed at two corners of the chamber. During this flushing period, all instruments sampled ambient air and were not connected to the chamber. The flushing period lasted at least 3 hours to ensure that the air composition in the chamber is the same as ambient composition. Secondly, we stopped both fans and connected all instruments to chamber. Because of the continued sampling by the instruments (~20 liter per minute) and the open corners of the chamber, ambient air continuously entered the chamber, even though the two fans were turned off. Thirdly, after sampling the chamber for about 30min, we injected a known amount of VOC (liquid) into the chamber with a needle, where the liquid vaporized upon injection. We continuously monitored the chamber composition for ~40 min after VOC injection. Lastly, we disconnected all instruments from the chamber, sampled ambient air, and turned on two fans to flush the chamber to prepare for the next perturbation experiment.

We perturbed the chamber content by injecting one of the following VOCs: isoprene, α-pinene, β-caryophyllene, *m*-xylene, or naphthalene, which are major biogenic or anthropogenic emissions, respectively. The injected VOC amounts were carefully selected. If the injection amount is too large, it is not atmospherically relevant, produces too much SOA, and will bias subsequent analysis. If the injection amount is too small, the produced SOA would fall below the detection limit of the experimental approach. The OA concentration in the chamber after perturbation ranges from 4 to 16 μg m^{-3}, which is within the range of typical ambient OA concentration. The VOC oxidation occurred in ambient air (inside the chamber) and lasted ~40 min. Several previous studies have used ambient air as background (Palm et al., 2017; Leungsakul et al., 2005). An important distinction between our study and pervious work is that we perturbed the ambient air only by injection of VOCs and no extra oxidant precursors (i.e., O_3, photolysis of H_2O and O_2, or photolysis of NO_x) were added to the chamber. Our approach allows for study of SOA formation from the specific VOCs injected and evaluate into which PMF factor the SOA is apportioned.

Each perturbation experiment can be divided into the following four periods: Amb_Bf (30min ambient measurement period before sampling chamber), Chamber_Bf (from sampling chamber to VOC injection, a period ~30min), Chamber_Af (from VOC injection to stop sampling chamber, a period ~40min), and Amb_Af (30min ambient measurement period after sampling chamber). We calculate the changes in the mass concentration of OA factors after perturbation based on the difference between Chamber_Bf and Chamber_Af, after taking ambient variation into account. The detailed procedure is presented in Appendix A. We develop a comprehensive set of criteria to determine if the changes are statistically significant and if the changes are simply due to ambient variations. The details of these criteria are also discussed in Appendix A.

2.2 Analytical instruments

A suite of analytical instruments was deployed to characterize both the gas-phase and particle-phase compositions. The particle-phase composition was monitored by a scanning mobility particle sizer (SMPS, TSI) and a high resolution time-of-flight aerosol mass spectrometer (HR-ToF-AMS, Aerodyne), which shared the same sampling line. A diaphragm pump (flow rate ~8 liter per minute) was connected to this sampling line, which increased the sampling flow rate and suppressed particle loss in the sampling line by reducing the residence time in the tubing. The HR-ToF-AMS measures the chemical composition and size distribution of submicron non-refractory species (NR-PM_1) with high temporal resolution. The instrument details about HR-ToF-AMS have been extensively discussed in the literature (Canagaratna et al., 2007; DeCarlo et al., 2006) and the operation of HR-ToF-AMS in this study is described in the section S2 of Supplement.

The gas-phase composition and oxidation products was monitored by an O_3 analyzer (Teledyne T400, lower detectable limit 0.6ppb), an ultrasensitive chemiluminescence NO_x monitor (Teledyne 200EU, lower detectable limit 50ppt), and a high-resolution time-of-flight chemical ionization mass spectrometer (HR-ToF-CIMS). The HR-ToF-CIMS with I^- as regent ion can measure a suite of oxygenated volatile organic compounds (oVOCs) at high frequency (1Hz). Detailed working principles and sampling protocol can be found in Lee et al. (2014). The concentrations of VOCs were not measured in this study. All gas-phase measurement instruments shared the same sampling line. Similar to the particle sampling line, a diaphragm pump (flow rate ~8 liter per minute) was connected to the gas sampling line to reduce the residence time in the tubing.

Atmos. Chem. Phys. Discuss., https://doi.org/10.5194/acp-2017-1109
Manuscript under review for journal Atmos. Chem. Phys.
Discussion started: 2 January 2018

156 **2.3 Positive Matrix Factorization (PMF) analysis**

157 PMF analysis has been widely used for aerosol source apportionment in the atmospheric chemistry
158 community (Jimenez et al., 2009; Crippa et al., 2014; Xu et al., 2015a; Ng et al., 2010; Ulbrich et
159 al., 2009; Beddows et al., 2015; Visser et al., 2015). PMF solves bilinear unmixing factor model
160 (Paatero and Tapper, 1994; Ulbrich et al., 2009) by minimizing the summed least squares errors
161 of the fit weighted with the error estimates of each measurement. We utilized the PMF2 solver,
162 which does not require a priori information and reduces subjectivity. In this study, we performed
163 PMF analysis on the high-resolution mass spectra of organic aerosol (inorganic species are
164 excluded) of combined ambient and perturbation data in the one-month measurements.
165 Considering that (1) the perturbation data only account for ~10% of total data and (2) the OA
166 concentration is similar in the perturbation experiments and typical ambient measurements, the
167 perturbation experiments do not create a new factor that does not already exist in the ambient data.
168 This is desirable because it allows PMF analysis to apportion the newly formed OA in the
169 perturbation experiments into pre-existing OA factors in the atmosphere.

170 We resolved five OA factors, including hydrocarbon-like OA (HOA), cooking OA (COA),
171 isoprene-derived OA (isoprene-OA), less-oxidized oxygenated OA (LO-OOA), and more-
172 oxidized oxygenated OA (MO-OOA). The time series and mass spectra of OA factors are shown
173 in Fig. 2. The same 5 factors have been identified at the same measurement site and extensively
174 discussed in the literature (Xu et al., 2015a; Xu et al., 2015b; Xu et al., 2017). Below, we only
175 provide a brief description on these OA factors and more details are discussed in section S3 of
176 Supplement. The mass spectrum of HOA is dominated by hydrocarbon-like ions ($C_xH_y^+$ ions) and
177 HOA is a surrogate of primary OA from vehicle emissions (Zhang et al., 2011). For COA, its
178 concentration is higher at meal times and its mass spectrum is characterized by prominent signal
179 at ions $C_3H_5^+$ (*m/z* 41) and $C_4H_7^+$ (*m/z* 55), which likely arise from unsaturated fatty acids (Huang
180 et al., 2010; Mohr et al., 2009). The mass spectrum of isoprene-OA is characterized by prominent
181 signal at ions $C_4H_5^+$ (*m/z* 53) and $C_5H_6O^+$ (*m/z* 82) and it is related the reactive uptake of isoprene
182 oxidation products, isoprene epoxydiols (IEPOX) (Budisulistiorini et al., 2013; Hu et al., 2015;
183 Robinson et al., 2011; Xu et al., 2015a). LO-OOA and MO-OOA are named based on their
184 differing carbon oxidation state.
185
186

2.4 Details of multiple ambient sampling sites

Measurements at multiple sites in the southeastern U.S. were performed as part of Southeastern Center for Air Pollution and Epidemiology study (SCAPE) and Southern Oxidant and Aerosol Study (SOAS). Detailed descriptions about these field studies have been discussed in the literature (Xu et al., 2015a; Xu et al., 2015b) and section S4 of Supplement. The sampling periods are shown in Table S1 and the sampling sites are briefly discussed below.

• Georgia Tech site (GT): This site is located on the rooftop of the Environmental Science and Technology building on the Georgia Institute of Technology (GT) campus, which is about 30-40m above the ground and 840m away from interstate I75/85. This is a representative urban site in Atlanta. This is also where the perturbation experiments in this study were conducted.

• Jefferson Street site (JST): This is a central SEARCH (SouthEastern Aerosol Research and Characterization) site, which is in Atlanta's urban area with a mixed commercial and residential neighborhood. It is about 2 km west of the GT site. The JST and GT sites are in the same grid cell in CMAQ.

• Yorkville site (YRK): This is a central SEARCH site located in a rural area in Georgia. This site is surrounded by agricultural land and forests and is at about 80 km northwest of JST site.

• Centreville site (CTR): This is a central SEARCH site in rural Alabama. The sampling site is surrounded by forests and away from large urban areas (55km SE and 84 km SW of Tuscaloosa and Birmingham, AL, respectively). The is the main ground site for the SOAS campaign.

2.5 Laboratory chamber study on SOA formation from α-pinene

To compare with results from the lab-in-the-field perturbation experiments, we performed laboratory experiments to study the SOA formation from α-pinene photooxidation under different NO_x conditions in the Georgia Tech Environmental Chamber (GTEC) facility. The facility consists of two 12 m^3 indoor Teflon chambers, which are suspended inside a temperature-controlled enclosure and surrounded by black lights. The detailed description about chamber facility can be found in Boyd et al. (2015). The experimental procedures have been discussed in Tuet et al. (2017). In brief, the chambers were flushed with clean air prior to each experiment. Then, α-pinene and oxidant sources (i.e., H_2O_2, NO_2, or HONO) were injected into chamber. Once the concentrations of species stabilize, the black lights were turned on to initiate photooxidation. The experimental conditions are summarized in Table S2. Considering that the OA mass concentration affects the

partitioning of semi-volatile organic compounds (Odum et al., 1996) and hence affects the organic mass spectra measured by AMS, we calculated the average mass spectra in these laboratory studies by only using the data when the OA mass concentration is below 10 μg m^{-3}, which is similar to that in our ambient perturbation experiments.

2.6 Community Multiscale Air Quality (CMAQ) Model

We used the Community Multiscale Air Quality (CMAQ) atmospheric chemical transport model to simulate the pollutant concentrations across the southeastern U.S. CMAQ v5.2gamma was run over the continental U.S. for time periods between May 2012 to July 2013 with 12km × 12km horizontal resolution. We focus our analysis on the southeastern U.S., which comprises 11 states (Arkansas, Alabama, Florida, Georgia, Kentucky, Louisiana, Mississippi, North Carolina, South Carolina, Tennessee, and Virginia). The meteorological inputs were generated with version 3.8 of the Weather Research and Forecasting model (WRF), Advanced Research WRF (ARW) core. We also applied lightning assimilation to improve convective rainfall (Heath et al., 2016). Anthropogenic emissions were based on the EPA (Environmental Protection Agency) NEI (National Emission Inventory) 2011 v2. Biogenic emissions were predicted by the BEIS (Biogenic Emission Inventory System) v3.6.1. The gas-phase chemistry was based on CB6r3 (Carbon Bond v6.3).

We performed two simulations with different organic aerosol treatment. The "default simulation" generally follows the scheme of Carlton et al. (2010), with IEPOX SOA following Pye et al. (2013) and documented in Appel et al. (2017) (Fig. S1a). The traditional two-product absorptive partitioning scheme (Odum et al., 1996) is used in "default simulation" to describe SOA formation from monoterpenes using data from laboratory experiments by Griffin et al. (1999). In the "updated simulation", we incorporate two recent findings. Firstly, we implemented MT+NO_3 chemistry to explicitly account for the organic nitrate compounds that have recently been shown to be a ubiquitous and important component of OA (Pye et al., 2015; Kiendler-Scharr et al., 2016; Lee et al., 2016; Ng et al., 2017). We follow the scheme described in Pye et al. (2015) to represent the formation and partition of organic nitrates from monoterpenes via multiple reaction pathways (i.e., oxidation by NO_3 and oxidation by OH/O_3 followed by RO_2+NO). Secondly, we improved the parameterization of SOA formation from MT+O_3/OH based on a recent study by Saha and Grieshop (2016), who applied a dual-thermodenuder system to study the α-pinene ozonolysis SOA. The authors extracted SOA yield parameters by using an evaporation-kinetics model and volatility

basis set (VBS). The SOA yields in Saha and Grieshop (2016) are consistent with recent findings on the formation of HOMs (Ehn et al., 2014; Zhang et al., 2015) and help to explain the observed slow evaporation of α-pinene SOA (Vaden et al., 2011). In the updated simulation, we use the VBS framework with parameters derived from Saha and Grieshop (2016). The properties of 7 volatility bins are listed in Table S3. A schematic of SOA treatment in "updated simulation" is shown in Fig. S1b. Additional details of the CMAQ simulations are given in the section S5 of Supplement.

3 Results and Discussions

3.1 α-pinene perturbation experiments

A total of 19 α-pinene perturbation experiments were performed at different times of the day (i.e., from 9am to 9pm) to probe a wide range of reaction conditions. The concentrations of O_3 and NO_x during α-pinene perturbation experiments are summarized in Table S4. Initially ~14 ppb α-pinene is injected into chamber, but only a small fraction of α-pinene is reacted in the chamber, with most of α-pinene being carried out of the chamber due to dilution with ambient air (section S6 of Supplement).

Fig. 3 shows the time series of OA factors in a typical α-pinene perturbation experiment. The most striking feature is a burst increase of LO-OOA after α-pinene injection. This is the most direct and compelling evidence that freshly formed α-pinene SOA contributes to LO-OOA. About 15 min after α-pinene injection, LO-OOA concentration starts to decrease, as ambient air continuously flows into the chamber and dilutes the concentration of LO-OOA (section S6 of Supplement). As shown in Fig. S2, the major known gas-phase oxidation products of α-pinene measured by HR-ToF-CIMS (Eddingsaas et al., 2012; Yu et al.; Lee et al., 2016) show an immediate increase after α-pinene injection. This verifies the rapid oxidation of α-pinene in the chamber.

Fig. 4a shows the perturbation-induced changes in the concentrations of OA factors for all α-pinene experiments. Out of 19 experiments, the LO-OOA concentration is enhanced in 14 experiments. Also, among all OA factors, LO-OOA shows the largest enhancement. This directly supports that freshly formed α-pinene SOA contributes to LO-OOA. The enhancement in LO-OOA concentration differs between experiments, mainly because the perturbations were performed at different times of day under different reaction conditions. Although the reaction

conditions vary between experiments, we note that both LO-OOA enhancement amount and LO-OOA formation rate (i.e., slope of LO-OOA increase) correlate positively with ozone concentration (Fig. 5). This correlation suggests that the concentration of oxidants, both ozone and hydroxy radical (OH, which is not measured in this study but is known to positively correlate with ozone in the atmosphere), is a controlling variable for OA formation in α-pinene experiments. This is likely because higher oxidant concentrations lead to more α-pinene consumption and hence more OA production with the same reaction time.

MO-OOA only increases in 1 out of 19 α-pinene experiments. The lack of enhancement in MO-OOA suggests that the HOMs, which are rapidly produced from the α-pinene oxidation (Ehn et al., 2014), are unlikely contributors to MO-OOA, though more future studies on the apportion of HOMs by PMF analysis are warranted. Isoprene-derived OA (isoprene-OA) increases in 7 out of 19 α-pinene experiments. This increase is surprising because the isoprene-OA factor is typically interpreted as SOA from the reactive uptake of IEPOX. Our results demonstrate that the isoprene-OA factor (also referred to as "IEPOX-OA" in some studies) could have interferences from α-pinene SOA. This conclusion could be applicable to isoprene-OA factor resolved at other monoterpenes-influenced sites. Primary OA factors, i.e., HOA and COA, only show slight increases in 1 or 2 α-pinene experiments, indicating a lack of interference from α-pinene SOA in these factors.

3.2 β-caryophyllene perturbation experiments

A total of 6 β-caryophyllene perturbation experiments were performed. Initially ~10 ppb β-caryophyllene is injected into chamber The concentrations of O_3 and NO_x during β-caryophyllene perturbation experiments are summarized in Table S4. In all β-caryophyllene perturbation experiments, LO-OOA also shows a significant enhancement (Fig. 4b). This clearly demonstrates that the freshly formed SOA from β-caryophyllene oxidation can be another source of LO-OOA. In addition to LO-OOA, COA shows an unexpected increase in 5 out of 6 β-caryophyllene experiments. We have ample evidence that the COA factor at the measurement site has contributions from cooking activities. Firstly, the diurnal variation of COA peaks during meal times (Fig. S3a). Secondly, the COA concentration shows clear increase on football days, consistent with barbecue activities on campus and close to the measurement site. Thirdly, the COA concentration is enhanced on the days right before the start of a new semester when there are many fraternity/sorority rush events (i.e., barbecue activities) on campus (Fig. S3b and S3c). However,

the COA enhancement in β-caryophyllene experiments underscores the fact that COA may not be purely from cooking activities in areas with large biogenic emissions.

3.3 Perturbation experiments with other VOCs

In addition to α-pinene and β-caryophyllene, we also performed perturbation experiments by injecting isoprene, *m*-xylene, or naphthalene, which are important biogenic and anthropogenic emissions, respectively. However, the SOA formation from these VOCs is not detectable. This is mainly due to either lower SOA yields (of isoprene) or slower oxidation rates (of *m*-xylene and naphthalene) compared to α-pinene and β-caryophyllene (section S6 of Supplement). The perturbation experiments with other VOCs confirm the stronger ability of α-pinene and β-caryophyllene to produce SOA (Kroll et al., 2006; Ng et al., 2007; Griffin et al., 1999).

We have also performed perturbation experiments by injecting acidic sulfate particles to probe reactive uptake of IEPOX. We observed enhancement in isoprene-OA concentration after the injection of sulfate particles. The detailed results are included in Appendix B.

3.4 Perturbation experiments vs. mass spectra comparison

The perturbation experiments provide more insights into the sources of OA factors than traditional mass spectra comparison. Previous studies concluded that LO-OOA (also denoted as semi-volatile oxygenated organic aerosol, SV-OOA) represents freshly formed SOA, mainly based on the observation that the mass spectra of laboratory-generated fresh SOA from various sources better resemble the mass spectrum of LO-OOA than other factors (Jimenez et al., 2009; Ng et al., 2010). While this mass spectra comparison approach sheds light on the potential sources of LO-OOA, it does not allow for evaluating whether freshly formed SOA in the atmosphere is exclusively apportioned into LO-OOA. The perturbation experiments, on the other hand, provide a way to evaluate this explicitly. Here, we directly produce SOA from a specific known VOC in ambient air matrix and determine where it is apportioned into. For example, we show that while fresh SOA from α-pinene and β-caryophyllene oxidations are mainly apportioned into LO-OOA, they could also be possibly apportioned into isoprene-OA factor and COA, respectively.

The perturbation experiments have the potential to utilize subtle differences across the entire the mass spectrum to evaluate the sources of OA factors. Based on previous laboratory studies, the mass spectra of fresh SOA from α-pinene oxidation and β-caryophyllene oxidation share much similarity, but there are subtle differences in the mass spectra (Bahreini et al., 2005;

Tasoglou and Pandis, 2015). For example, in the perturbation experiments a fraction of the fresh β-caryophyllene SOA is apportioned into COA factor, but we do not observe similar behavior for α-pinene SOA. This is likely because f_{55} (i.e., the ratio of *m/z* 55 to total signal in the mass spectrum) is typically higher in β-caryophyllene SOA than α-pinene SOA and the mass spectrum of COA is characterized by prominent signal at *m/z* 55 (Fig. 2).

3.5 Connection between laboratory and field studies

Due to the difficulties associated with accurately measuring complex chemical processes in the atmosphere, laboratory studies have been an integral part in our understanding of atmospheric chemistry (Burkholder et al., 2017). However, the representativeness of laboratory studies under simplified conditions with respect to the complex atmosphere is difficult to evaluate. One unique feature of our lab-in-the-field approach is that the VOC oxidation and SOA formation proceed under realistic atmospheric conditions. Taking advantage of this, we provide a direct link between laboratory studies and ambient observations. Previous laboratory studies have shown that NO can affect SOA composition by influencing the fate of organic peroxy radical (RO_2, a critical radical intermediate formed from VOC oxidation) (Kroll and Seinfeld, 2008; Sarrafzadeh et al., 2016; Presto et al., 2005). To evaluate the representativeness of laboratory studies and directly investigate the effects of NO on SOA composition, in Fig. 6, we compare the chemical composition of α-pinene SOA formed in laboratory studies under different NO conditions (denoted as SOA_{lab}) with those in α-pinene ambient perturbation experiments (denoted as $SOA_{ambient}$). The degree of similarity in OA mass spectra (i.e., evaluated by the correlation coefficient) between laboratory α-pinene SOA generated under NO-free condition (i.e., denoted as $SOA_{lab,NO\text{-}free}$, using H_2O_2 photolysis as oxidant source) and $SOA_{ambient}$ shows a strong dependence on ambient NO concentration, under which the $SOA_{ambient}$ is formed. The degree of similarity in mass spectra decreases rapidly when ambient NO increases from 0.1 to 0.2ppb, and then reaches a plateau at ~0.3ppb NO. The opposite trend is observed when laboratory α-pinene SOA generated in the presence of high NO concentrations (i.e., denoted as $SOA_{lab,high\text{-}NO}$, using the photolysis of NO_2 or nitrous acid as oxidant source) are compared with $SOA_{ambient}$. These observations directly demonstrate the transition of RO_2 fate as a function of NO under ambient conditions. For the perturbation experiments performed when ambient NO is below ~0.1ppb, the mass spectra of $SOA_{ambient}$ are similar to $SOA_{lab,NO\text{-}free}$, consistent with that RO_2 mainly reacts with hydroperoxyl (HO_2) or isomerizes. In contrast, for the perturbation experiments performed when ambient NO is

above ~0.3ppb, the mass spectra of $SOA_{ambient}$ are similar to $SOA_{lab,high\text{-}NO}$, consistent with that the RO_2 fate is dominated by NO. This NO level (~0.3ppb) is consistent with the NO level required to dominate the fate of RO_2 in the atmosphere, as calculated by using previously measured HO_2 and kinetic rate constants (section S8 of Supplement). These observations also directly illustrate that the SOA composition from laboratory studies can be representative of atmosphere. We note that the mass spectra of $SOA_{ambient}$ are generally more similar with that of laboratory SOA generated using NO_2 photolysis as oxidant source than using nitrous acid photolysis. This suggests that laboratory experiments using NO_2 photolysis as oxidant source better represent ambient high NO oxidation conditions in the southeastern U.S. than experiments using nitrous acid do. Possible explanations are discussed in section S7 of Supplement. This finding provides new insights into designing future laboratory experiments to better mimic the oxidations in ambient environments.

3.6 Abundance of SOA_{MT+SQT} in the Southeastern U.S.

The ambient perturbation experiments provide direct evidence that the majority of freshly formed SOA from the oxidation of MT and SQT contributes to LO-OOA. Previous studies suggest that the oxidation of β-pinene (another important monoterpene) by nitrate radicals (NO_3) contributes to LO-OOA in the southeastern U.S. (Boyd et al., 2015; Xu et al., 2015a), though this reaction alone cannot replicate the magnitude of LO-OOA, particularly during the daytime (Pye et al., 2015). Considering the large biogenic emissions in the southeastern U.S. (Guenther et al., 2012) and the new results from our perturbation experiments, we propose that the major source of LO-OOA in this region is the oxidation of MT and SQT by various oxidants (O_3, OH, and NO_3). To test this hypothesis, we use CMAQ to simulate pollutant concentrations across the southeastern U.S.

The SOA_{MT+SQT} concentration in the default simulation (i.e., no explicit organic nitrate partitioning, Griffin et al. (1999) photooxidation parameterization) is significantly lower than LO-OOA by 55-84% (Fig. 7). In contrast, SOA_{MT+SQT} in the updated simulation (explicit organic nitrates and Saha and Grieshop (2016) VBS for MT+O_3/OH) accurately reproduces the magnitude and diurnal variability of LO-OOA for each site (Fig. 8a). The model bias is reduced to within ~20% for most sites, except for Centreville, Alabama (i.e., 43% for CTR_June dataset). The consistency between modeled SOA_{MT+SQT} and measured LO-OOA at multiple sites and in different seasons supports our hypothesis that LO-OOA largely arises from the oxidation of MT and SQT in the southeastern U.S. Fig. 8b present maps of ground-level SOA_{MT+SQT} concentration

401 corresponding to the time periods of observational data. The SOA_{MT+SQT} concentration is
402 substantially higher in the southeast than other U.S. regions. The SOA_{MT+SQT} is present throughout
403 the year and reaches the largest concentration in summer. The spatial and seasonal variation of
404 SOA_{MT+SQT} concentration is consistent with MT and SQT emissions (Guenther et al., 2012). The
405 annual concentration of SOA_{MT+SQT} in $PM_{2.5}$ in the southeastern U.S. is ~2.1 μg m^{-3} (i.e., average
406 concentration over the six sampling periods and over the southeastern U.S. in the updated
407 simulation). This accounts for 21% of World Health Organization $PM_{2.5}$ guideline (i.e., 10 μg m^{-3}
408 annual mean) and indicates a significant contributor of environmental risk to the 77 million
409 habitants in the southeastern U.S. Also, the estimated concentration of SOA_{MT+SQT} is substantially
410 higher than represented in current models (Lane et al., 2008; Zheng et al., 2015). The oxidation of
411 MT and SQT is likely an under-estimated contributor to natural PM in pre-industrial period, which
412 determines the baseline state of atmosphere and the estimate of climate forcing by anthropogenic
413 emissions (Carslaw et al., 2013). Models need to improve the description of the MT and SQT
414 oxidation to reduce the uncertainties in estimated OA budget and subsequent climate forcing.
415 We note that we do not conclude that LO-OOA arises exclusively from MT and SQT, SOA
416 from anthropogenic VOCs may also contribute to LO-OOA. However, the SOA contribution from
417 anthropogenic VOCs is expected to be much smaller than that from biogenic monoterpenes and
418 sesquiterpenes in the southeastern U.S. Firstly, as shown in the perturbation experiments, α-pinene
419 and β-caryophyllene produce more SOA than *m*-xylene and naphthalene using the same
420 experimental approach in ambient air matrix. Together with weaker emissions of anthropogenic
421 VOCs than biogenic VOCs in the southeastern U.S. (Goldstein et al., 2009), the small contribution
422 to SOA from anthropogenic VOCs is expected. Secondly, as indicated in Fig. S5, the modeled
423 concentration of SOA from anthropogenic VOCs is on the order of 0.1 μg m^{-3}. Even if we double
424 the SOA yields of anthropogenic VOCs to account for the potential vapor wall loss in laboratory
425 studies (Zhang et al., 2014), the concentration of SOA from anthropogenic VOCs oxidation is still
426 negligible compared to SOA_{MT+SQT}. SOA from anthropogenic VOCs oxidation could be abundant
427 in urban areas of the western U.S. There is evidence that LO-OOA in California is related to the
428 oxidation of anthropogenic VOCs, as radiocarbon analysis suggests 68-75% of carbon in LO-OOA
429 in California stems from fossil sources (Hayes et al., 2013; Zotter et al., 2014). The contribution
430 from anthropogenic VOCs to LO-OOA awaits exploration through ambient perturbation
431 experiments in various locations around the world.

Atmos. Chem. Phys. Discuss., https://doi.org/10.5194/acp-2017-1109
Manuscript under review for journal Atmos. Chem. Phys.
Discussion started: 2 January 2018

4 Implications

In this study, we propose that LO-OOA can be used as a surrogate of fresh SOA from MT and SQT in the southeastern U.S., based on the weight of evidence provided by: (1) the large emissions of MT and SQT in this region; (2) the contribution from MT + NO_3 to LO-OOA as shown in previous studies; (3) perturbation experiments providing direct evidence that the majority of fresh SOA from the oxidation of MT and SQT contributes to LO-OOA; (4) the consistency of modeled SOA_{MT+SQT} with the magnitude and diurnal trend of LO-OOA at different sites and in different seasons.

Using LO-OOA as a surrogate of SOA_{MT+SQT} in the southeastern U.S., our ambient ground measurements suggest that at least 19-34% of OA in the southeastern U.S. is from the oxidation of biogenic monoterpenes and sesquiterpenes (Xu et al., 2015a). The fraction of biogenic OA in the southeastern U.S. is even larger if we consider that isoprene-OA could account for 21-36% of OA in summer (albeit potential interferences of SOA from monoterpenes oxidation) and that MO-OOA (24-49% of OA) likely contains SOA from long-term photochemical oxidation of biogenic VOCs. The dominant biogenic origin of SOA poses a challenge to control its burden in the southeastern U.S., if the roles of anthropogenic oxidants and other controlling factors are not recognized. Previous studies have shown that the SOA formation from biogenic VOCs can be mediated by anthropogenic emissions, such as nitrogen oxides and sulfur dioxide (Hoyle et al., 2011; Goldstein et al., 2009; Surratt et al., 2010; Rollins et al., 2012; Xu et al., 2015a). Thus, regulating anthropogenic emissions could help reduce SOA concentration (Lane et al., 2008; Pye et al., 2015; Zheng et al., 2015). For example, as observed in our ambient perturbation experiments, one controlling parameter of α-pinene SOA formation is the concentration of atmospheric oxidants (O_3, OH, and NO_3), which are known to strongly depend on NO_x concentration. As it has been shown that anthropogenic emissions exert complex and non-linear influences on biogenic SOA formation (Zheng et al., 2015), the effectiveness of regulating anthropogenic emissions on biogenic SOA burden requires careful investigations. Importantly, the novel lab-in-the-field perturbation experiments substantially improve our understanding of ambient OA sources. This approach is easily applicable to other regions in the world. Future experiments conducted under various ambient environments and with diverse SOA precursors would facilitate accurate quantification of global OA sources as well as their climate and health impacts.

Atmos. Chem. Phys. Discuss., https://doi.org/10.5194/acp-2017-1109
Manuscript under review for journal Atmos. Chem. Phys.
Discussion started: 2 January 2018

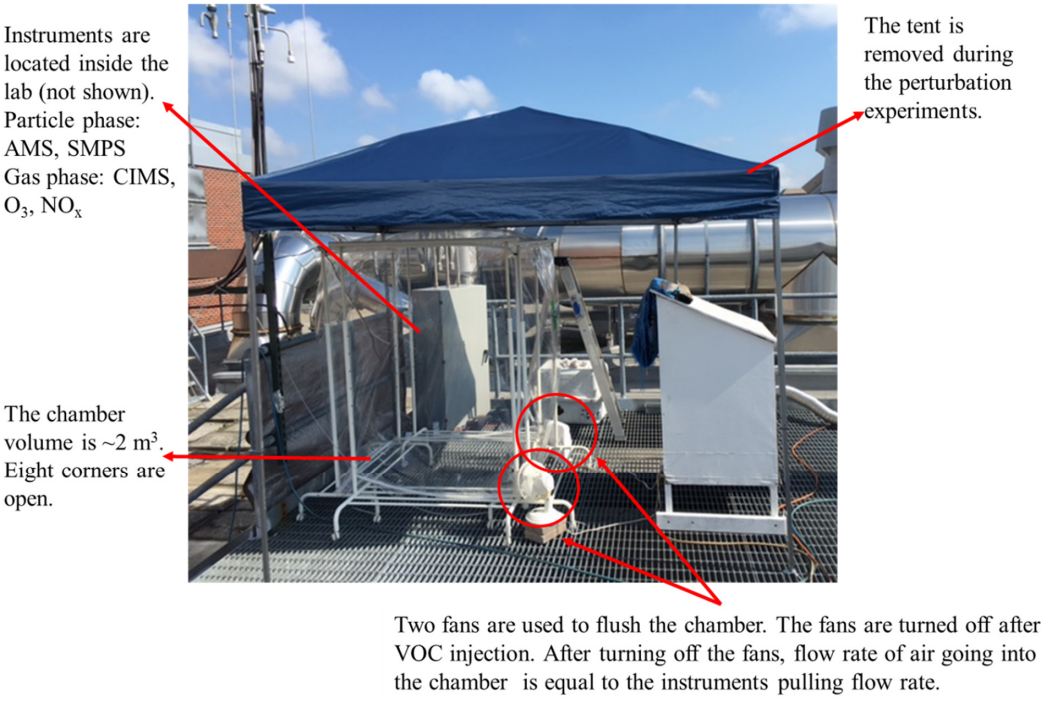

Fig. 1. The instrument setup for ambient perturbation experiments.

Atmos. Chem. Phys. Discuss., https://doi.org/10.5194/acp-2017-1109
Manuscript under review for journal Atmos. Chem. Phys.
Discussion started: 2 January 2018

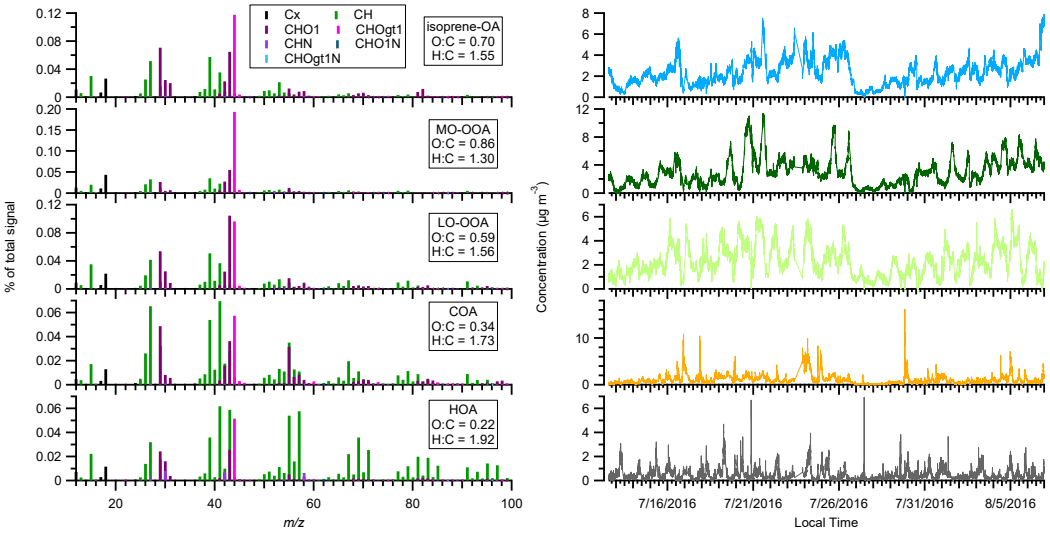

Fig. 2. The mass spectra and time series of OA factors in perturbation study. The time series includes both the ambient data and perturbation experiments data.

Atmos. Chem. Phys. Discuss., https://doi.org/10.5194/acp-2017-1109
Manuscript under review for journal Atmos. Chem. Phys.
Discussion started: 2 January 2018

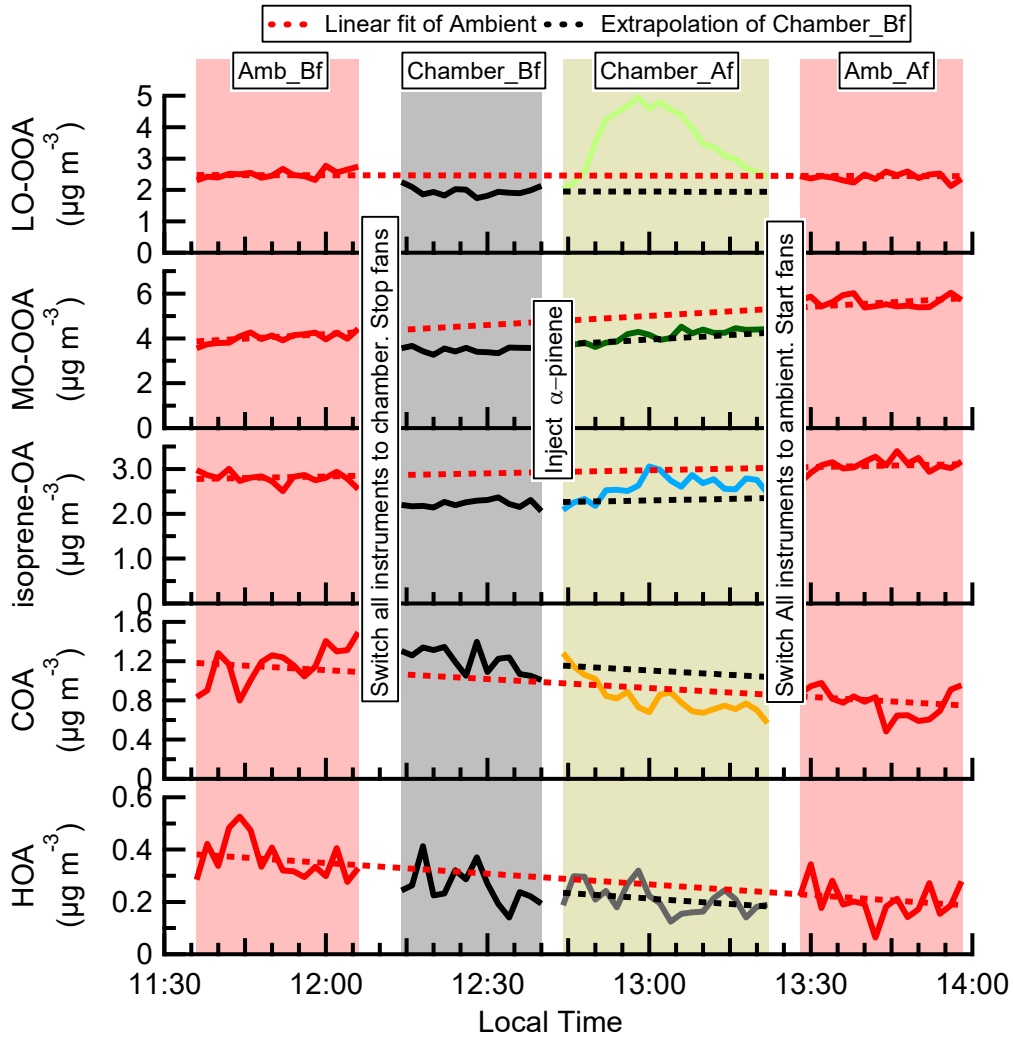

Fig. 3. The time series of OA factors in an α-pinene perturbation experiment (Expt ID: ap_0801_1). Each perturbation experiment includes four periods: Amb_Bf (~30min), Chamber_Bf (~30min), Chamber_Af (~40min), and Amb_Af (~40min). "Amb" and "Chamber" represent that instruments are sampling ambient and chamber, respectively. "Bf" and "Af" stand for before and after perturbation, respectively. The solid lines are measurement data. The dashed red lines are the linear fits of ambient data (i.e., combined Amb_Bf and Amb_Af). The slopes are used to extrapolate Chamber_Bf data to Chamber_Af period (i.e., dashed black lines). The validity of the linearity assumption is discussed in Appendix A. The difference between measurements (i.e., solid lines) and extrapolated Chamber_Bf (i.e., dashed black lines) represents the change caused by perturbation.

Atmos. Chem. Phys. Discuss., https://doi.org/10.5194/acp-2017-1109
Manuscript under review for journal Atmos. Chem. Phys.
Discussion started: 2 January 2018

Atmospheric Chemistry and Physics Discussions

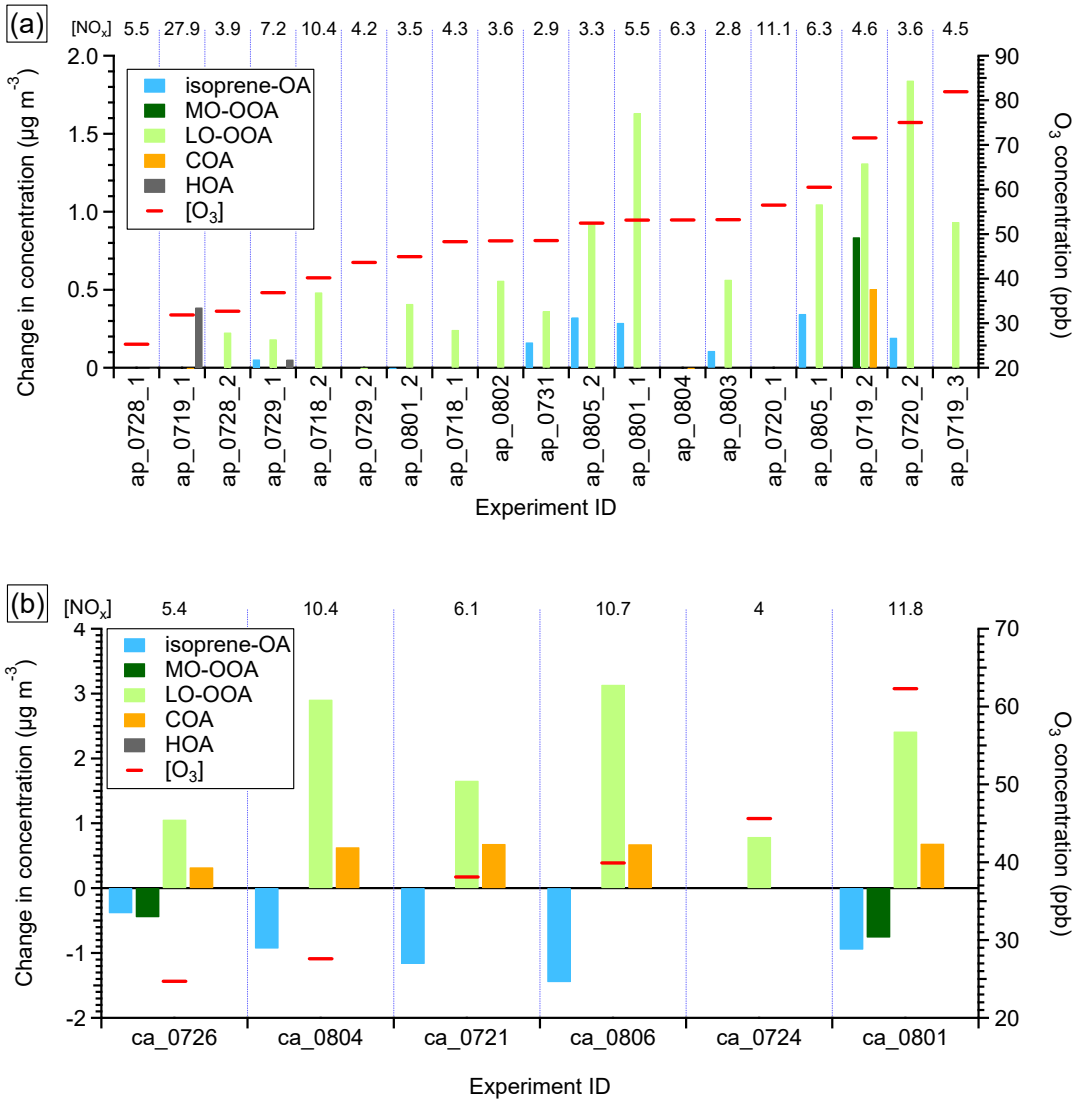

Fig. 4. The statistically significant changes in the concentrations of OA factors after perturbation by (a) α-pinene and (b) β-caryophyllene. The experiments are sorted by average [O_3] during Chamber_Af. The average [NO_x] during Chamber_Af are shown on top of the figure. The changes in concentration are the differences between measurements during Chamber_Af and extrapolated Chamber_Bf (Appendix A). A set of criteria are developed to evaluate if the changes are statistically significant and if the changes are due to ambient variation (Appendix A). Isoprene-OA decreases after β-caryophyllene injection. The reason for this decrease is unclear, but likely due to the limitations of PMF analysis, which assumes constant mass spectra of OA factors over time (section S9 of Supplement).

Atmos. Chem. Phys. Discuss., https://doi.org/10.5194/acp-2017-1109
Manuscript under review for journal Atmos. Chem. Phys.
Discussion started: 2 January 2018

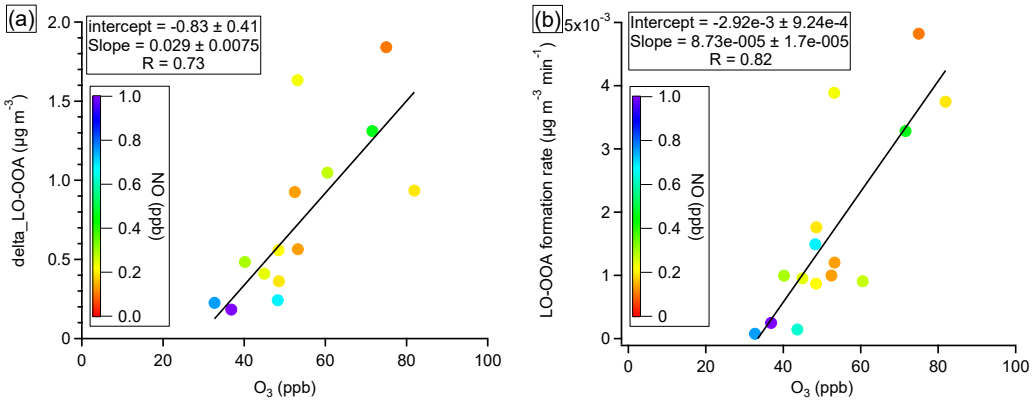

Fig. 5. Observations of trends in (a) LO-OOA enhancement amount and (b) LO-OOA formation rate with O_3 concentration in α-pinene perturbation experiments. The data points are colored by average NO concentration during Chamber_Af period. The slopes, intercepts, and correlation coefficients (R) are obtained by least square fit.

Atmos. Chem. Phys. Discuss., https://doi.org/10.5194/acp-2017-1109
Manuscript under review for journal Atmos. Chem. Phys.
Discussion started: 2 January 2018

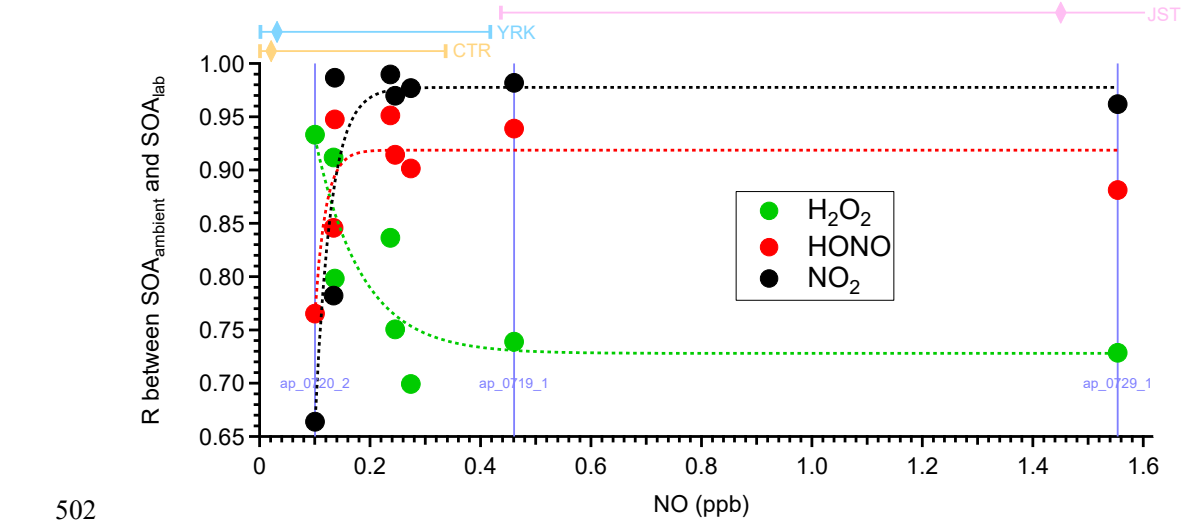

Fig. 6. The correlation coefficients between the mass spectra of OA formed in laboratory under different NO conditions ("SOA_{lab}") and those of OA formed in ambient α-pinene perturbation experiments ("$SOA_{ambient}$"). The subscripts "$_{lab}$" and "$_{ambient}$" indicate the SOA formed under laboratory conditions and ambient conditions, respectively. Three different oxidant sources (i.e., H_2O_2, HONO, and NO_2) are used to create different NO concentrations in laboratory studies. The mass spectra of "$SOA_{ambient}$" are calculated by comparing the mass spectra of OA during Chamber_Af and those of extrapolated Chamber_Bf (section S7 of Supplement). To calculate reliable mass spectra of "$SOA_{ambient}$", only the experiments with significant OA enhancement are analyzed and shown here (Appendix A). The x-axis is the average NO concentration during each perturbation experiment. The data points on the same vertical line (i.e., the same NO concentration) are from the same perturbation experiment, but compared to three different laboratory experiments. The dashed lines are used to guide eyes. The bars on top of the figure represent the 10th, 50th, and 90th percentiles of NO concentration for CTR (Centreville, AL), YRK (Yorkville, GA), and JST (Jefferson Street, GA) in 2013. The NO concentration is measured by the SouthEastern Aerosol Research and Characterization (SEARCH) network. The 90th percentile of NO concentration in JST is 14.8 ppb, which is not shown in the figure.

Atmos. Chem. Phys. Discuss., https://doi.org/10.5194/acp-2017-1109
Manuscript under review for journal Atmos. Chem. Phys.
Discussion started: 2 January 2018

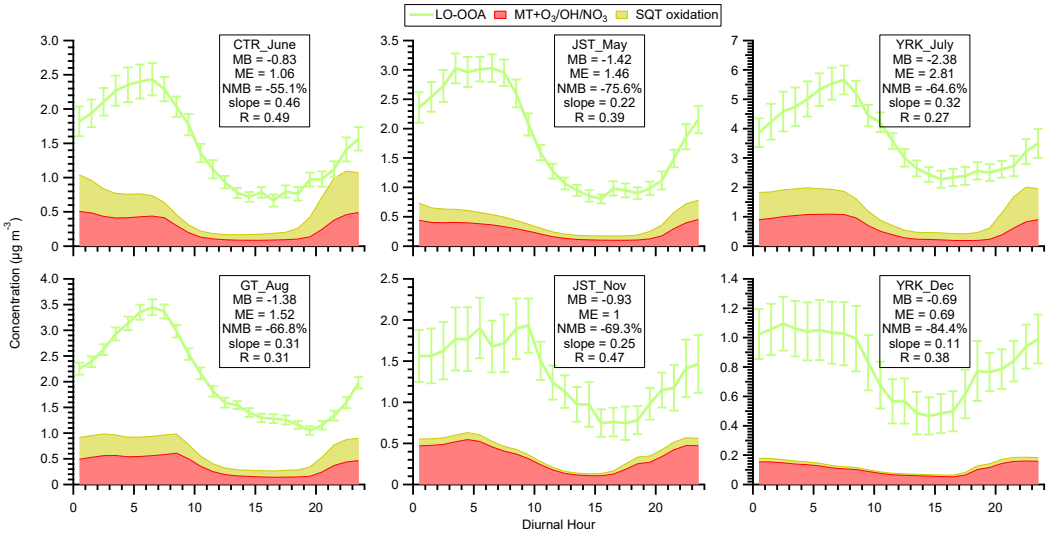

Fig. 7. The diurnal trends of LO-OOA and modeled SOA from monoterpenes and sesquiterpenes at different sampling sites in the southeastern U.S. in the default simulation. The mean bias (MB), mean error (ME), and normalized mean bias (NMB) are shown for each site. The slopes and R are obtained by least square fit.

Atmos. Chem. Phys. Discuss., https://doi.org/10.5194/acp-2017-1109
Manuscript under review for journal Atmos. Chem. Phys.
Discussion started: 2 January 2018

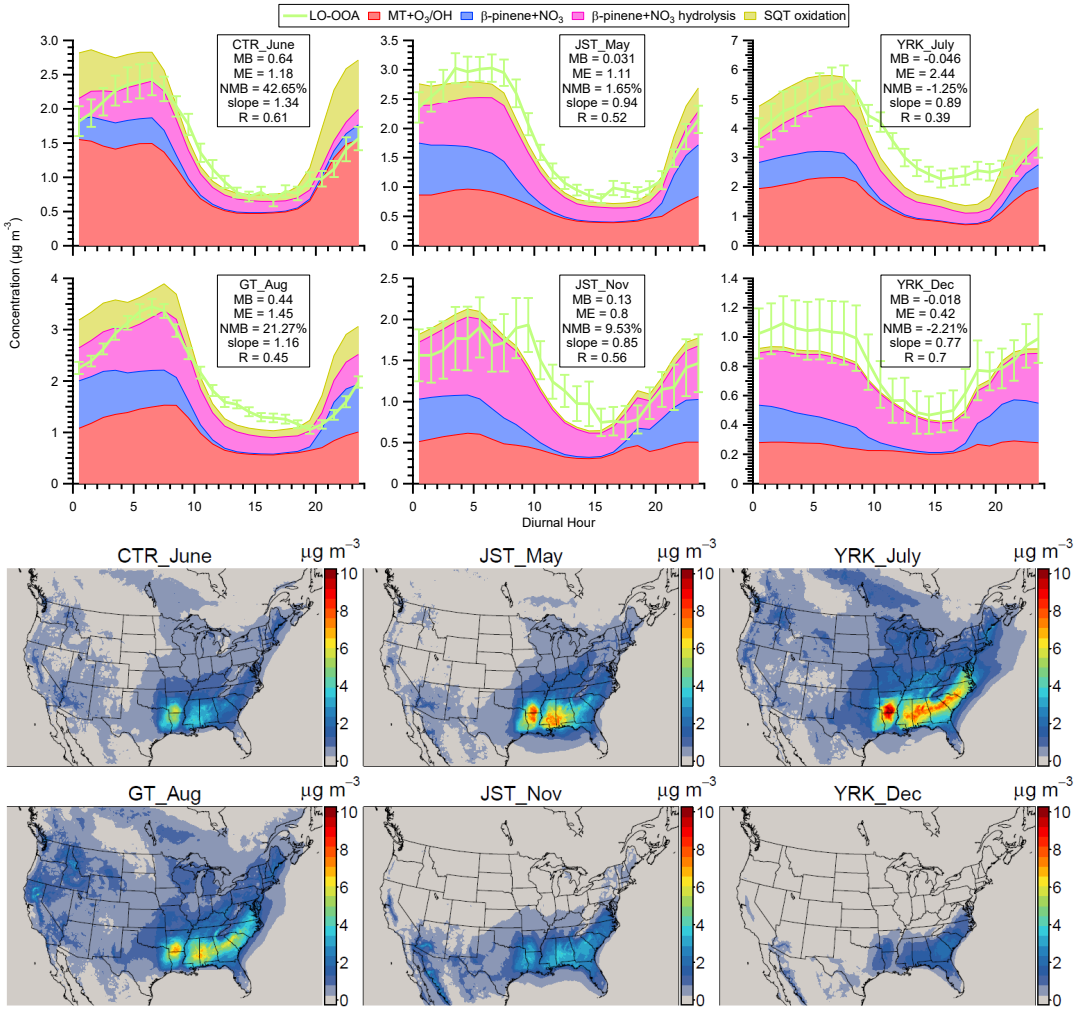

Fig. 8. (a) top panel: the diurnal trends of LO-OOA and modeled SOA from monoterpenes and sesquiterpenes (SOA_{MT+SQT}) at different sampling sites in the southeastern U.S. (b) bottom panel: maps of modeled ground-level SOA_{MT+SQT} concentration. Model results shown here are from the updated simulation. Abbreviations correspond to Centreville (CTR), Jefferson Street (JST), Yorkville (YRK), Georgia Institute of Technology (GT). Detailed sampling periods are shown in Table S1. In panel (a), since the perturbation experiments show that 16% of SOA from α-pinene oxidation is apportioned into isoprene-OA (Fig. S7a), we only include 84% of modeled SOA from $MT+O_3/OH$ when comparing with LO-OOA for the sites with isoprene-OA (Fig. S7a). The mean bias (MB), mean error (ME), and normalized mean bias (NMB) for each site are shown in each panel. The slopes and correlation coefficients (R) are obtained by least square fit. The error bars indicate the standard error. In panel (b), average SOA_{MT+SQT} concentration in $PM_{2.5}$ during each sampling period is reported.

Acknowledgments

L.X. and N.L.N. acknowledged support from US Environmental Protection Agency (EPA) STAR Grant RD-83540301, and National Science Foundation (NSF) grants 1555034 and 1455588. The HR-ToF-CIMS was purchased with NSF Major Research Instrumentation (MRI) grant 1428738. HOTP contributions were supported by a Presidential Early Career Award for Scientists and Engineers (PECASE). The authors thank R. J. Weber and M. R. Canagaratna for helpful discussions, the SEARCH personnel for their many contributions, the CSRA for preparing emissions and meteorology for CMAQ simulations. The US EPA through its Office of Research and Development supported the research described here. It has been subjected to Agency administrative review and approved for publication but may not necessarily reflect official Agency policy.

551 **References**

552

553 Appel, K. W., Napelenok, S. L., Foley, K. M., Pye, H. O. T., Hogrefe, C., Luecken, D. J., Bash, J.
554 O., Roselle, S. J., Pleim, J. E., Foroutan, H., Hutzell, W. T., Pouliot, G. A., Sarwar, G., Fahey, K.
555 M., Gantt, B., Gilliam, R. C., Heath, N. K., Kang, D., Mathur, R., Schwede, D. B., Spero, T. L.,
556 Wong, D. C., and Young, J. O.: Description and evaluation of the Community Multiscale Air
557 Quality (CMAQ) modeling system version 5.1, Geosci. Model Dev., 10, 1703-1732,
558 10.5194/gmd-10-1703-2017, 2017.
559
560 Bahreini, R., Keywood, M. D., Ng, N. L., Varutbangkul, V., Gao, S., Flagan, R. C., Seinfeld, J.
561 H., Worsnop, D. R., and Jimenez, J. L.: Measurements of secondary organic aerosol from oxidation
562 of cycloalkenes, terpenes, and m-xylene using an Aerodyne aerosol mass spectrometer, Environ
563 Sci Technol, 39, 5674-5688, Doi 10.1021/Es048061a, 2005.
564
565 Beddows, D. C. S., Harrison, R. M., Green, D. C., and Fuller, G. W.: Receptor modelling of both
566 particle composition and size distribution from a background site in London, UK, Atmos. Chem.
567 Phys., 15, 10107-10125, 10.5194/acp-15-10107-2015, 2015.
568
569 Boyd, C. M., Sanchez, J., Xu, L., Eugene, A. J., Nah, T., Tuet, W. Y., Guzman, M. I., and Ng, N.
570 L.: Secondary organic aerosol formation from the β-pinene+NO3 system: effect of humidity and
571 peroxy radical fate, Atmos. Chem. Phys., 15, 7497-7522, 10.5194/acp-15-7497-2015, 2015.
572
573 Budisulistiorini, S. H., Canagaratna, M. R., Croteau, P. L., Marth, W. J., Baumann, K., Edgerton,
574 E. S., Shaw, S. L., Knipping, E. M., Worsnop, D. R., Jayne, J. T., Gold, A., and Surratt, J. D.:
575 Real-Time Continuous Characterization of Secondary Organic Aerosol Derived from Isoprene
576 Epoxydiols in Downtown Atlanta, Georgia, Using the Aerodyne Aerosol Chemical Speciation
577 Monitor, Environ Sci Technol, 47, 5686-5694, Doi 10.1021/Es400023n, 2013.
578
579 Budisulistiorini, S. H., Li, X., Bairai, S. T., Renfro, J., Liu, Y., Liu, Y. J., McKinney, K. A., Martin,
580 S. T., McNeill, V. F., Pye, H. O. T., Nenes, A., Neff, M. E., Stone, E. A., Mueller, S., Knote, C.,
581 Shaw, S. L., Zhang, Z., Gold, A., and Surratt, J. D.: Examining the effects of anthropogenic
582 emissions on isoprene-derived secondary organic aerosol formation during the 2013 Southern
583 Oxidant and Aerosol Study (SOAS) at the Look Rock, Tennessee ground site, Atmos. Chem. Phys.,
584 15, 8871-8888, 10.5194/acp-15-8871-2015, 2015.
585
586 Burkholder, J. B., Abbatt, J. P. D., Barnes, I., Roberts, J. M., Melamed, M. L., Ammann, M.,
587 Bertram, A. K., Cappa, C. D., Carlton, A. M. G., Carpenter, L. J., Crowley, J. N., Dubowski, Y.,
588 George, C., Heard, D. E., Herrmann, H., Keutsch, F. N., Kroll, J. H., McNeill, V. F., Ng, N. L.,
589 Nizkorodov, S. A., Orlando, J. J., Percival, C. J., Picquet-Varrault, B., Rudich, Y., Seakins, P. W.,
590 Surratt, J. D., Tanimoto, H., Thornton, J. A., Zhu, T., Tyndall, G. S., Wahner, A., Weschler, C. J.,
591 Wilson, K. R., and Ziemann, P. J.: The Essential Role for Laboratory Studies in Atmospheric
592 Chemistry, Environ Sci Technol, 10.1021/acs.est.6b04947, 2017.
593
594 Canagaratna, M. R., Jayne, J. T., Jimenez, J. L., Allan, J. D., Alfarra, M. R., Zhang, Q., Onasch,
595 T. B., Drewnick, F., Coe, H., Middlebrook, A., Delia, A., Williams, L. R., Trimborn, A. M.,
596 Northway, M. J., DeCarlo, P. F., Kolb, C. E., Davidovits, P., and Worsnop, D. R.: Chemical and

597 microphysical characterization of ambient aerosols with the aerodyne aerosol mass spectrometer,
598 Mass Spectrometry Reviews, 26, 185-222, 10.1002/mas.20115, 2007.
599
600 Canonaco, F., Crippa, M., Slowik, J. G., Baltensperger, U., and Prévôt, A. S. H.: SoFi, an IGOR-
601 based interface for the efficient use of the generalized multilinear engine (ME-2) for the source
602 apportionment: ME-2 application to aerosol mass spectrometer data, Atmos. Meas. Tech., 6, 3649-
603 3661, 10.5194/amt-6-3649-2013, 2013.
604
605 Carlton, A. G., Bhave, P. V., Napelenok, S. L., Edney, E. O., Sarwar, G., Pinder, R. W., Pouliot,
606 G. A., and Houyoux, M.: Model Representation of Secondary Organic Aerosol in CMAQv4.7,
607 Environ Sci Technol, 44, 8553-8560, 10.1021/es100636q, 2010.
608
609 Carslaw, K. S., Lee, L. A., Reddington, C. L., Pringle, K. J., Rap, A., Forster, P. M., Mann, G. W.,
610 Spracklen, D. V., Woodhouse, M. T., Regayre, L. A., and Pierce, J. R.: Large contribution of
611 natural aerosols to uncertainty in indirect forcing, Nature, 503, 67-71, Doi 10.1038/Nature12674,
612 2013.
613
614 Crippa, M., Canonaco, F., Lanz, V. A., Äijälä, M., Allan, J. D., Carbone, S., Capes, G., Ceburnis,
615 D., Dall'Osto, M., Day, D. A., DeCarlo, P. F., Ehn, M., Eriksson, A., Freney, E., Hildebrandt Ruiz,
616 L., Hillamo, R., Jimenez, J. L., Junninen, H., Kiendler-Scharr, A., Kortelainen, A. M., Kulmala,
617 M., Laaksonen, A., Mensah, A. A., Mohr, C., Nemitz, E., O'Dowd, C., Ovadnevaite, J., Pandis, S.
618 N., Petäjä, T., Poulain, L., Saarikoski, S., Sellegri, K., Swietlicki, E., Tiitta, P., Worsnop, D. R.,
619 Baltensperger, U., and Prévôt, A. S. H.: Organic aerosol components derived from 25 AMS data
620 sets across Europe using a consistent ME-2 based source apportionment approach, Atmos. Chem.
621 Phys., 14, 6159-6176, 10.5194/acp-14-6159-2014, 2014.
622
623 DeCarlo, P. F., Kimmel, J. R., Trimborn, A., Northway, M. J., Jayne, J. T., Aiken, A. C., Gonin,
624 M., Fuhrer, K., Horvath, T., Docherty, K. S., Worsnop, D. R., and Jimenez, J. L.: Field-Deployable,
625 High-Resolution, Time-of-Flight Aerosol Mass Spectrometer, Anal Chem, 78, 8281-8289,
626 10.1021/ac061249n, 2006.
627
628 Eddingsaas, N. C., Loza, C. L., Yee, L. D., Seinfeld, J. H., and Wennberg, P. O.: α-pinene
629 photooxidation under controlled chemical conditions – Part 1: Gas-phase composition in low- and
630 high-NO_x environments, Atmos. Chem. Phys., 12, 6489-6504, 10.5194/acp-12-
631 6489-2012, 2012.
632
633 Ehn, M., Thornton, J. A., Kleist, E., Sipila, M., Junninen, H., Pullinen, I., Springer, M., Rubach,
634 F., Tillmann, R., Lee, B., Lopez-Hilfiker, F., Andres, S., Acir, I.-H., Rissanen, M., Jokinen, T.,
635 Schobesberger, S., Kangasluoma, J., Kontkanen, J., Nieminen, T., Kurten, T., Nielsen, L. B.,
636 Jorgensen, S., Kjaergaard, H. G., Canagaratna, M., Maso, M. D., Berndt, T., Petaja, T., Wahner,
637 A., Kerminen, V.-M., Kulmala, M., Worsnop, D. R., Wildt, J., and Mentel, T. F.: A large source
638 of low-volatility secondary organic aerosol, Nature, 506, 476-479, 10.1038/nature13032, 2014.
639
640 Goldstein, A. H., Koven, C. D., Heald, C. L., and Fung, I. Y.: Biogenic carbon and anthropogenic
641 pollutants combine to form a cooling haze over the southeastern United States, Proceedings of the
642 National Academy of Sciences, 106, 8835-8840, 10.1073/pnas.0904128106, 2009.

643
644 Griffin, R. J., Cocker, D. R., Flagan, R. C., and Seinfeld, J. H.: Organic aerosol formation from
645 the oxidation of biogenic hydrocarbons, J Geophys Res-Atmos, 104, 3555-3567, Doi
646 10.1029/1998jd100049, 1999.
647
648 Guenther, A., Jiang, X., Heald, C. L., Sakulyanontvittaya, T., Duhl, T., Emmons, L. K., and Wang,
649 X.: The Model of Emissions of Gases and Aerosols from Nature version 2.1 (MEGAN2.1): an
650 extended and updated framework for modeling biogenic emissions, Geosci. Model Dev., 5, 1471-
651 1492, 10.5194/gmd-5-1471-2012, 2012.
652
653 Hallquist, M., Wenger, J. C., Baltensperger, U., Rudich, Y., Simpson, D., Claeys, M., Dommen,
654 J., Donahue, N. M., George, C., Goldstein, A. H., Hamilton, J. F., Herrmann, H., Hoffmann, T.,
655 Iinuma, Y., Jang, M., Jenkin, M. E., Jimenez, J. L., Kiendler-Scharr, A., Maenhaut, W., McFiggans,
656 G., Mentel, T. F., Monod, A., Prevot, A. S. H., Seinfeld, J. H., Surratt, J. D., Szmigielski, R., and
657 Wildt, J.: The formation, properties and impact of secondary organic aerosol: current and emerging
658 issues, Atmos Chem Phys, 9, 5155-5236, 2009.
659
660 Hayes, P. L., Ortega, A. M., Cubison, M. J., Froyd, K. D., Zhao, Y., Cliff, S. S., Hu, W. W.,
661 Toohey, D. W., Flynn, J. H., Lefer, B. L., Grossberg, N., Alvarez, S., Rappenglueck, B., Taylor, J.
662 W., Allan, J. D., Holloway, J. S., Gilman, J. B., Kuster, W. C., De Gouw, J. A., Massoli, P., Zhang,
663 X., Liu, J., Weber, R. J., Corrigan, A. L., Russell, L. M., Isaacman, G., Worton, D. R., Kreisberg,
664 N. M., Goldstein, A. H., Thalman, R., Waxman, E. M., Volkamer, R., Lin, Y. H., Surratt, J. D.,
665 Kleindienst, T. E., Offenberg, J. H., Dusanter, S., Griffith, S., Stevens, P. S., Brioude, J., Angevine,
666 W. M., and Jimenez, J. L.: Organic aerosol composition and sources in Pasadena, California,
667 during the 2010 CalNex campaign, J Geophys Res-Atmos, 118, 9233-9257, Doi
668 10.1002/Jgrd.50530, 2013.
669
670 Heath, N. K., Pleim, J. E., Gilliam, R. C., and Kang, D.: A simple lightning assimilation technique
671 for improving retrospective WRF simulations, Journal of Advances in Modeling Earth Systems, 8,
672 1806-1824, 10.1002/2016MS000735, 2016.
673
674 Hennigan, C. J., Bergin, M. H., Russell, A. G., Nenes, A., and Weber, R. J.: Gas/particle
675 partitioning of water-soluble organic aerosol in Atlanta, Atmos Chem Phys, 9, 3613-3628, 2009.
676
677 Hodzic, A., Kasibhatla, P. S., Jo, D. S., Cappa, C. D., Jimenez, J. L., Madronich, S., and Park, R.
678 J.: Rethinking the global secondary organic aerosol (SOA) budget: stronger production, faster
679 removal, shorter lifetime, Atmos. Chem. Phys., 16, 7917-7941, 10.5194/acp-16-7917-2016, 2016.
680
681 Hoyle, C. R., Boy, M., Donahue, N. M., Fry, J. L., Glasius, M., Guenther, A., Hallar, A. G., Hartz,
682 K. H., Petters, M. D., Petaja, T., Rosenoern, T., and Sullivan, A. P.: A review of the anthropogenic
683 influence on biogenic secondary organic aerosol, Atmos Chem Phys, 11, 321-343, DOI
684 10.5194/acp-11-321-2011, 2011.
685
686 Hu, W. W., Campuzano-Jost, P., Palm, B. B., Day, D. A., Ortega, A. M., Hayes, P. L., Krechmer,
687 J. E., Chen, Q., Kuwata, M., Liu, Y. J., de Sá, S. S., McKinney, K., Martin, S. T., Hu, M.,
688 Budisulistiorini, S. H., Riva, M., Surratt, J. D., St. Clair, J. M., Isaacman-Van Wertz, G., Yee, L.

D., Goldstein, A. H., Carbone, S., Brito, J., Artaxo, P., de Gouw, J. A., Koss, A., Wisthaler, A., Mikoviny, T., Karl, T., Kaser, L., Jud, W., Hansel, A., Docherty, K. S., Alexander, M. L., Robinson, N. H., Coe, H., Allan, J. D., Canagaratna, M. R., Paulot, F., and Jimenez, J. L.: Characterization of a real-time tracer for isoprene epoxydiols-derived secondary organic aerosol (IEPOX-SOA) from aerosol mass spectrometer measurements, Atmos. Chem. Phys., 15, 11807-11833, 10.5194/acp-15-11807-2015, 2015.

Huang, X. F., He, L. Y., Hu, M., Canagaratna, M. R., Sun, Y., Zhang, Q., Zhu, T., Xue, L., Zeng, L. W., Liu, X. G., Zhang, Y. H., Jayne, J. T., Ng, N. L., and Worsnop, D. R.: Highly time-resolved chemical characterization of atmospheric submicron particles during 2008 Beijing Olympic Games using an Aerodyne High-Resolution Aerosol Mass Spectrometer, Atmos Chem Phys, 10, 8933-8945, DOI 10.5194/acp-10-8933-2010, 2010.

Jimenez, J. L., Canagaratna, M. R., Donahue, N. M., Prevot, A. S. H., Zhang, Q., Kroll, J. H., DeCarlo, P. F., Allan, J. D., Coe, H., Ng, N. L., Aiken, A. C., Docherty, K. S., Ulbrich, I. M., Grieshop, A. P., Robinson, A. L., Duplissy, J., Smith, J. D., Wilson, K. R., Lanz, V. A., Hueglin, C., Sun, Y. L., Tian, J., Laaksonen, A., Raatikainen, T., Rautiainen, J., Vaattovaara, P., Ehn, M., Kulmala, M., Tomlinson, J. M., Collins, D. R., Cubison, M. J., Dunlea, E. J., Huffman, J. A., Onasch, T. B., Alfarra, M. R., Williams, P. I., Bower, K., Kondo, Y., Schneider, J., Drewnick, F., Borrmann, S., Weimer, S., Demerjian, K., Salcedo, D., Cottrell, L., Griffin, R., Takami, A., Miyoshi, T., Hatakeyama, S., Shimono, A., Sun, J. Y., Zhang, Y. M., Dzepina, K., Kimmel, J. R., Sueper, D., Jayne, J. T., Herndon, S. C., Trimborn, A. M., Williams, L. R., Wood, E. C., Middlebrook, A. M., Kolb, C. E., Baltensperger, U., and Worsnop, D. R.: Evolution of Organic Aerosols in the Atmosphere, Science, 326, 1525-1529, DOI 10.1126/science.1180353, 2009.

Kiendler-Scharr, A., Mensah, A. A., Friese, E., Topping, D., Nemitz, E., Prevot, A. S. H., Äijälä, M., Allan, J., Canonaco, F., Canagaratna, M., Carbone, S., Crippa, M., Dall Osto, M., Day, D. A., De Carlo, P., Di Marco, C. F., Elbern, H., Eriksson, A., Freney, E., Hao, L., Herrmann, H., Hildebrandt, L., Hillamo, R., Jimenez, J. L., Laaksonen, A., McFiggans, G., Mohr, C., O'Dowd, C., Otjes, R., Ovadnevaite, J., Pandis, S. N., Poulain, L., Schlag, P., Sellegri, K., Swietlicki, E., Tiitta, P., Vermeulen, A., Wahner, A., Worsnop, D., and Wu, H. C.: Ubiquity of organic nitrates from nighttime chemistry in the European submicron aerosol, Geophysical Research Letters, 43, 7735-7744, 10.1002/2016GL069239, 2016.

Kroll, J. H., Ng, N. L., Murphy, S. M., Varutbangkul, V., Flagan, R. C., and Seinfeld, J. H.: Chamber studies of secondary organic aerosol growth by reactive uptake of simple carbonyl compounds, J Geophys Res-Atmos, 110, Doi 10.1029/2005jd006004, 2005.

Kroll, J. H., Ng, N. L., Murphy, S. M., Flagan, R. C., and Seinfeld, J. H.: Secondary organic aerosol formation from isoprene photooxidation, Environ Sci Technol, 40, 1869-1877, Doi 10.1021/Es0524301, 2006.

Kroll, J. H., and Seinfeld, J. H.: Chemistry of secondary organic aerosol: Formation and evolution of low-volatility organics in the atmosphere, Atmospheric Environment, 42, 3593-3624, DOI 10.1016/j.atmosenv.2008.01.003, 2008.

735 Lane, T. E., Donahue, N. M., and Pandis, S. N.: Effect of NOx on Secondary Organic Aerosol
736 Concentrations, Environ Sci Technol, 42, 6022-6027, 10.1021/es703225a, 2008.
737
738 Lee, B. H., Lopez-Hilfiker, F. D., Mohr, C., Kurtén, T., Worsnop, D. R., and Thornton, J. A.: An
739 Iodide-Adduct High-Resolution Time-of-Flight Chemical-Ionization Mass Spectrometer:
740 Application to Atmospheric Inorganic and Organic Compounds, Environ Sci Technol, 48, 6309-
741 6317, 10.1021/es500362a, 2014.
742
743 Lee, B. H., Mohr, C., Lopez-Hilfiker, F. D., Lutz, A., Hallquist, M., Lee, L., Romer, P., Cohen, R.
744 C., Iyer, S., Kurtén, T., Hu, W., Day, D. A., Campuzano-Jost, P., Jimenez, J. L., Xu, L., Ng, N. L.,
745 Guo, H., Weber, R. J., Wild, R. J., Brown, S. S., Koss, A., de Gouw, J., Olson, K., Goldstein, A.
746 H., Seco, R., Kim, S., McAvey, K., Shepson, P. B., Starn, T., Baumann, K., Edgerton, E. S., Liu,
747 J., Shilling, J. E., Miller, D. O., Brune, W., Schobesberger, S., D'Ambro, E. L., and Thornton, J.
748 A.: Highly functionalized organic nitrates in the southeast United States: Contribution to secondary
749 organic aerosol and reactive nitrogen budgets, Proceedings of the National Academy of Sciences,
750 113, 1516-1521, 10.1073/pnas.1508108113, 2016.
751
752 Lelieveld, J., Evans, J. S., Fnais, M., Giannadaki, D., and Pozzer, A.: The contribution of outdoor
753 air pollution sources to premature mortality on a global scale, Nature, 525, 367-371,
754 10.1038/nature15371, 2015.
755
756 Leungsakul, S., Jeffries, H. E., and Kamens, R. M.: A kinetic mechanism for predicting secondary
757 aerosol formation from the reactions of d-limonene in the presence of oxides of nitrogen and
758 natural sunlight, Atmospheric Environment, 39, 7063-7082,
759 https://doi.org/10.1016/j.atmosenv.2005.08.024, 2005.
760
761 Liu, Y., Kuwata, M., McKinney, K. A., and Martin, S. T.: Uptake and release of gaseous species
762 accompanying the reactions of isoprene photo-oxidation products with sulfate particles, Phys
763 Chem Chem Phys, 18, 1595-1600, 10.1039/C5CP04551G, 2016.
764
765 Mohr, C., Huffman, J. A., Cubison, M. J., Aiken, A. C., Docherty, K. S., Kimmel, J. R., Ulbrich,
766 I. M., Hannigan, M., and Jimenez, J. L.: Characterization of Primary Organic Aerosol Emissions
767 from Meat Cooking, Trash Burning, and Motor Vehicles with High-Resolution Aerosol Mass
768 Spectrometry and Comparison with Ambient and Chamber Observations, Environ Sci Technol,
769 43, 2443-2449, 10.1021/es8011518, 2009.
770
771 Ng, N. L., Kroll, J. H., Chan, A. W. H., Chhabra, P. S., Flagan, R. C., and Seinfeld, J. H.: Secondary
772 organic aerosol formation from m-xylene, toluene, and benzene, Atmos. Chem. Phys., 7, 3909-
773 3922, 10.5194/acp-7-3909-2007, 2007.
774
775 Ng, N. L., Canagaratna, M. R., Zhang, Q., Jimenez, J. L., Tian, J., Ulbrich, I. M., Kroll, J. H.,
776 Docherty, K. S., Chhabra, P. S., Bahreini, R., Murphy, S. M., Seinfeld, J. H., Hildebrandt, L.,
777 Donahue, N. M., DeCarlo, P. F., Lanz, V. A., Prevot, A. S. H., Dinar, E., Rudich, Y., and Worsnop,
778 D. R.: Organic aerosol components observed in Northern Hemispheric datasets from Aerosol Mass
779 Spectrometry, Atmos Chem Phys, 10, 4625-4641, DOI 10.5194/acp-10-4625-2010, 2010.
780

781 Ng, N. L., Brown, S. S., Archibald, A. T., Atlas, E., Cohen, R. C., Crowley, J. N., Day, D. A.,
782 Donahue, N. M., Fry, J. L., Fuchs, H., Griffin, R. J., Guzman, M. I., Herrmann, H., Hodzic, A.,
783 Iinuma, Y., Jimenez, J. L., Kiendler-Scharr, A., Lee, B. H., Luecken, D. J., Mao, J., McLaren, R.,
784 Mutzel, A., Osthoff, H. D., Ouyang, B., Picquet-Varrault, B., Platt, U., Pye, H. O. T., Rudich, Y.,
785 Schwantes, R. H., Shiraiwa, M., Stutz, J., Thornton, J. A., Tilgner, A., Williams, B. J., and Zaveri,
786 R. A.: Nitrate radicals and biogenic volatile organic compounds: oxidation, mechanisms, and
787 organic aerosol, Atmos. Chem. Phys., 17, 2103-2162, 10.5194/acp-17-2103-2017, 2017.
788
789 Odum, J. R., Hoffmann, T., Bowman, F., Collins, D., Flagan, R. C., and Seinfeld, J. H.:
790 Gas/Particle Partitioning and Secondary Organic Aerosol Yields, Environ Sci Technol, 30, 2580-
791 2585, 10.1021/es950943+, 1996.
792
793 Paatero, P., and Tapper, U.: Positive Matrix Factorization - a Nonnegative Factor Model with
794 Optimal Utilization of Error-Estimates of Data Values, Environmetrics, 5, 111-126, DOI
795 10.1002/env.3170050203, 1994.
796
797 Paatero, P.: The Multilinear Engine—A Table-Driven, Least Squares Program for Solving
798 Multilinear Problems, Including the n-Way Parallel Factor Analysis Model, Journal of
799 Computational and Graphical Statistics, 8, 854-888, 10.1080/10618600.1999.10474853, 1999.
800
801 Palm, B. B., de Sá, S. S., Day, D. A., Campuzano-Jost, P., Hu, W., Seco, R., Sjostedt, S. J., Park,
802 J. H., Guenther, A. B., Kim, S., Brito, J., Wurm, F., Artaxo, P., Thalman, R., Wang, J., Yee, L. D.,
803 Wernis, R., Isaacman-VanWertz, G., Goldstein, A. H., Liu, Y., Springston, S. R., Souza, R.,
804 Newburn, M. K., Alexander, M. L., Martin, S. T., and Jimenez, J. L.: Secondary organic aerosol
805 formation from ambient air in an oxidation flow reactor in central Amazonia, Atmos. Chem. Phys.
806 Discuss., 2017, 1-56, 10.5194/acp-2017-795, 2017.
807
808 Presto, A. A., Huff Hartz, K. E., and Donahue, N. M.: Secondary Organic Aerosol Production
809 from Terpene Ozonolysis. 2. Effect of NOx Concentration, Environ Sci Technol, 39, 7046-7054,
810 10.1021/es050400s, 2005.
811
812 Pye, Pinder, R. W., Piletic, I. R., Xie, Y., Capps, S. L., Lin, Y. H., Surratt, J. D., Zhang, Z. F.,
813 Gold, A., Luecken, D. J., Hutzell, W. T., Jaoui, M., Offenberg, J. H., Kleindienst, T. E.,
814 Lewandowski, M., and Edney, E. O.: Epoxide Pathways Improve Model Predictions of Isoprene
815 Markers and Reveal Key Role of Acidity in Aerosol Formation, Environ Sci Technol, 47, 11056-
816 11064, Doi 10.1021/Es402106h, 2013.
817
818 Pye, H. O. T., Chan, A. W. H., Barkley, M. P., and Seinfeld, J. H.: Global modeling of organic
819 aerosol: the importance of reactive nitrogen (NOx and NO3), Atmos Chem Phys, 10, 11261-11276,
820 DOI 10.5194/acp-10-11261-2010, 2010.
821
822 Pye, H. O. T., Luecken, D. J., Xu, L., Boyd, C. M., Ng, N. L., Baker, K. R., Ayres, B. R., Bash, J.
823 O., Baumann, K., Carter, W. P. L., Edgerton, E., Fry, J. L., Hutzell, W. T., Schwede, D. B., and
824 Shepson, P. B.: Modeling the Current and Future Roles of Particulate Organic Nitrates in the
825 Southeastern United States, Environ Sci Technol, 49, 14195-14203, 10.1021/acs.est.5b03738,
826 2015.

827
828 Robinson, N. H., Hamilton, J. F., Allan, J. D., Langford, B., Oram, D. E., Chen, Q., Docherty, K.,
829 Farmer, D. K., Jimenez, J. L., Ward, M. W., Hewitt, C. N., Barley, M. H., Jenkin, M. E., Rickard,
830 A. R., Martin, S. T., McFiggans, G., and Coe, H.: Evidence for a significant proportion of
831 Secondary Organic Aerosol from isoprene above a maritime tropical forest, Atmos Chem Phys,
832 11, 1039-1050, DOI 10.5194/acp-11-1039-2011, 2011.
833
834 Rollins, A. W., Browne, E. C., Min, K.-E., Pusede, S. E., Wooldridge, P. J., Gentner, D. R.,
835 Goldstein, A. H., Liu, S., Day, D. A., Russell, L. M., and Cohen, R. C.: Evidence for NOx Control
836 over Nighttime SOA Formation, Science, 337, 1210-1212, 10.1126/science.1221520, 2012.
837
838 Saha, P. K., and Grieshop, A. P.: Exploring Divergent Volatility Properties from Yield and
839 Thermodenuder Measurements of Secondary Organic Aerosol from α-Pinene Ozonolysis, Environ
840 Sci Technol, 10.1021/acs.est.6b00303, 2016.
841
842 Sarrafzadeh, M., Wildt, J., Pullinen, I., Springer, M., Kleist, E., Tillmann, R., Schmitt, S. H., Wu,
843 C., Mentel, T. F., Zhao, D., Hastie, D. R., and Kiendler-Scharr, A.: Impact of NOx and OH on
844 secondary organic aerosol formation from β-pinene photooxidation, Atmos. Chem. Phys., 16,
845 11237-11248, 10.5194/acp-16-11237-2016, 2016.
846
847 Sen, P. K.: Estimates of the Regression Coefficient Based on Kendall's Tau, Journal of the
848 American Statistical Association, 63, 1379-1389, 10.1080/01621459.1968.10480934, 1968.
849
850 Spracklen, D. V., Jimenez, J. L., Carslaw, K. S., Worsnop, D. R., Evans, M. J., Mann, G. W.,
851 Zhang, Q., Canagaratna, M. R., Allan, J., Coe, H., McFiggans, G., Rap, A., and Forster, P.: Aerosol
852 mass spectrometer constraint on the global secondary organic aerosol budget, Atmos. Chem. Phys.,
853 11, 12109-12136, 10.5194/acp-11-12109-2011, 2011.
854
855 Surratt, J. D., Chan, A. W. H., Eddingsaas, N. C., Chan, M. N., Loza, C. L., Kwan, A. J., Hersey,
856 S. P., Flagan, R. C., Wennberg, P. O., and Seinfeld, J. H.: Reactive intermediates revealed in
857 secondary organic aerosol formation from isoprene, P Natl Acad Sci USA, 107, 6640-6645, DOI
858 10.1073/pnas.0911114107, 2010.
859
860 Tasoglou, A., and Pandis, S. N.: Formation and chemical aging of secondary organic aerosol
861 during the β-caryophyllene oxidation, Atmos. Chem. Phys., 15, 6035-6046, 10.5194/acp-15-6035-
862 2015, 2015.
863
864 Tsigaridis, K., Daskalakis, N., Kanakidou, M., Adams, P. J., Artaxo, P., Bahadur, R., Balkanski,
865 Y., Bauer, S. E., Bellouin, N., Benedetti, A., Bergman, T., Berntsen, T. K., Beukes, J. P., Bian, H.,
866 Carslaw, K. S., Chin, M., Curci, G., Diehl, T., Easter, R. C., Ghan, S. J., Gong, S. L., Hodzic, A.,
867 Hoyle, C. R., Iversen, T., Jathar, S., Jimenez, J. L., Kaiser, J. W., Kirkevåg, A., Koch, D., Kokkola,
868 H., Lee, Y. H., Lin, G., Liu, X., Luo, G., Ma, X., Mann, G. W., Mihalopoulos, N., Morcrette, J. J.,
869 Müller, J. F., Myhre, G., Myriokefalitakis, S., Ng, N. L., O'Donnell, D., Penner, J. E., Pozzoli, L.,
870 Pringle, K. J., Russell, L. M., Schulz, M., Sciare, J., Seland, Ø., Shindell, D. T., Sillman, S., Skeie,
871 R. B., Spracklen, D., Stavrakou, T., Steenrod, S. D., Takemura, T., Tiitta, P., Tilmes, S., Tost, H.,
872 van Noije, T., van Zyl, P. G., von Salzen, K., Yu, F., Wang, Z., Wang, Z., Zaveri, R. A., Zhang,

H., Zhang, K., Zhang, Q., and Zhang, X.: The AeroCom evaluation and intercomparison of organic aerosol in global models, Atmos. Chem. Phys., 14, 10845-10895, 10.5194/acp-14-10845-2014, 2014.

Tuet, W. Y., Chen, Y., Xu, L., Fok, S., Gao, D., Weber, R. J., and Ng, N. L.: Chemical oxidative potential of secondary organic aerosol (SOA) generated from the photooxidation of biogenic and anthropogenic volatile organic compounds, Atmos. Chem. Phys., 17, 839-853, 10.5194/acp-17-839-2017, 2017.

Ulbrich, I. M., Canagaratna, M. R., Zhang, Q., Worsnop, D. R., and Jimenez, J. L.: Interpretation of organic components from Positive Matrix Factorization of aerosol mass spectrometric data, Atmos. Chem. Phys., 9, 2891-2918, 10.5194/acp-9-2891-2009, 2009.

Vaden, T. D., Imre, D., Beránek, J., Shrivastava, M., and Zelenyuk, A.: Evaporation kinetics and phase of laboratory and ambient secondary organic aerosol, Proceedings of the National Academy of Sciences, 108, 2190-2195, 10.1073/pnas.1013391108, 2011.

Verma, V., Fang, T., Guo, H., King, L., Bates, J. T., Peltier, R. E., Edgerton, E., Russell, A. G., and Weber, R. J.: Reactive oxygen species associated with water-soluble PM2.5 in the southeastern United States: spatiotemporal trends and source apportionment, Atmos. Chem. Phys., 14, 12915-12930, 10.5194/acp-14-12915-2014, 2014.

Visser, S., Slowik, J. G., Furger, M., Zotter, P., Bukowiecki, N., Canonaco, F., Flechsig, U., Appel, K., Green, D. C., Tremper, A. H., Young, D. E., Williams, P. I., Allan, J. D., Coe, H., Williams, L. R., Mohr, C., Xu, L., Ng, N. L., Nemitz, E., Barlow, J. F., Halios, C. H., Fleming, Z. L., Baltensperger, U., and Prévôt, A. S. H.: Advanced source apportionment of size-resolved trace elements at multiple sites in London during winter, Atmos. Chem. Phys., 15, 11291-11309, 10.5194/acp-15-11291-2015, 2015.

Xu, L., Guo, H., Boyd, C. M., Klein, M., Bougiatioti, A., Cerully, K. M., Hite, J. R., Isaacman-VanWertz, G., Kreisberg, N. M., Knote, C., Olson, K., Koss, A., Goldstein, A. H., Hering, S. V., de Gouw, J., Baumann, K., Lee, S.-H., Nenes, A., Weber, R. J., and Ng, N. L.: Effects of anthropogenic emissions on aerosol formation from isoprene and monoterpenes in the southeastern United States, Proceedings of the National Academy of Sciences, 112, 37-42, 10.1073/pnas.1417609112, 2015a.

Xu, L., Suresh, S., Guo, H., Weber, R. J., and Ng, N. L.: Aerosol characterization over the southeastern United States using high-resolution aerosol mass spectrometry: spatial and seasonal variation of aerosol composition and sources with a focus on organic nitrates, Atmos. Chem. Phys., 15, 7307-7336, 10.5194/acp-15-7307-2015, 2015b.

Xu, L., Middlebrook, A. M., Liao, J., de Gouw, J. A., Guo, H., Weber, R. J., Nenes, A., Lopez-Hilfiker, F. D., Lee, B. H., Thornton, J. A., Brock, C. A., Neuman, J. A., Nowak, J. B., Pollack, I. B., Welti, A., Graus, M., Warneke, C., and Ng, N. L.: Enhanced formation of isoprene-derived organic aerosol in sulfur-rich power plant plumes during Southeast Nexus, Journal of Geophysical Research: Atmospheres, 121, 11,137-111,153, 10.1002/2016JD025156, 2016.

Yu, J., Cocker, D. R., Griffin, R. J., Flagan, R. C., and Seinfeld, J. H.: Gas-Phase Ozone Oxidation of Monoterpenes: Gaseous and Particulate Products, J Atmos Chem, 34, 207-258, 10.1023/a:1006254930583,

Zhang, X., Cappa, C. D., Jathar, S. H., McVay, R. C., Ensberg, J. J., Kleeman, M. J., and Seinfeld, J. H.: Influence of vapor wall loss in laboratory chambers on yields of secondary organic aerosol, Proceedings of the National Academy of Sciences, 10.1073/pnas.1404727111, 2014.

Zhang, X., McVay, R. C., Huang, D. D., Dalleska, N. F., Aumont, B., Flagan, R. C., and Seinfeld, J. H.: Formation and evolution of molecular products in α-pinene secondary organic aerosol, Proceedings of the National Academy of Sciences, 112, 14168-14173, 10.1073/pnas.1517742112, 2015.

Zheng, Y., Unger, N., Hodzic, A., Emmons, L., Knote, C., Tilmes, S., Lamarque, J. F., and Yu, P.: Limited effect of anthropogenic nitrogen oxides on secondary organic aerosol formation, Atmos. Chem. Phys., 15, 13487-13506, 10.5194/acp-15-13487-2015, 2015.

Zotter, P., El-Haddad, I., Zhang, Y., Hayes, P. L., Zhang, X., Lin, Y.-H., Wacker, L., Schnelle-Kreis, J., Abbaszade, G., Zimmermann, R., Surratt, J. D., Weber, R., Jimenez, J. L., Szidat, S., Baltensperger, U., and Prévôt, A. S. H.: Diurnal cycle of fossil and nonfossil carbon using radiocarbon analyses during CalNex, Journal of Geophysical Research: Atmospheres, 119, 2013JD021114, 10.1002/2013JD021114, 2014.

Atmos. Chem. Phys. Discuss., https://doi.org/10.5194/acp-2017-1109
Manuscript under review for journal Atmos. Chem. Phys.
Discussion started: 2 January 2018

Atmospheric Chemistry and Physics Discussions

Appendix A. Data Analysis Method for Perturbation Experiments

The most challenging and important analysis is to determine if the perturbation results in a statistically significant change in the mass concentration of OA factors. We perform the following analysis to calculate the changes in the mass concentration of OA factors after perturbation, to determine if the change is significant, and to evaluate if the change is simply due to ambient variation.

The duration of one perturbation experiment is about 130min, including four periods: Amb_Bf (~30min), Chamber_Bf (~30min), Chamber_Af (~40min), and Amb_Af (~30min), as illustrated in Fig. A1. Firstly, we assume that the ambient variation is linear during both the Chamber_Bf and Chamber_Af periods (i.e., when instruments are connected to chamber and not sampling the ambient aerosol) and that the ambient variation can be represented by interpolating Amb_Bf and Amb_Af. The validity of this assumption will be discussed shortly. To obtain the slope of ambient variation, we analyze the combined Amb_Bf and Amb_Af data and use Theil-Sen estimator(Sen, 1968). The Theil-Sen estimator is a method to robustly fit a line to a set of two-dimensional points (i.e., concentration "*C*" and time "*t*" in this study). This method chooses the median of the slopes $(C_j\text{-}C_i)/(t_j\text{-}t_i)$ determined by all pairs of sample points. Compared to simple linear regression using ordinary least squares, the Theil-Sen estimator is robust and insensitive to outliers. Unless specifically noted, the slope is Appendix A is calculated from Theil-Sen estimator. Secondly, we use the slope to extrapolate the Chamber_Bf data to estimate aerosol concentration inside the chamber during the Chamber_Af period if there were no VOC injection. We refer to this estimated aerosol concentration as "extrapolated Chamber_Bf" and use it as the reference to calculate the change in aerosol mass concentration after perturbation. We extrapolate the Chamber_Bf data, instead of ambient data, because the OA concentration in chamber is lower than that in the atmosphere due to wall loss. Thirdly, we calculate the changes in the concentration of OA factors based on the difference between measured Chamber_Af data and "extrapolated Chamber_Bf".

For each perturbation experiment, after calculating the changes in the concentration of OA factors, we develop a set of criteria to determine if the changes are statistically significant and if the changes are simply due to ambient variation. The increase in the concentration of an OA factor needs to satisfy all criteria to be considered as statistically significant and not due to ambient variation.

Criterion 1: The difference in concentration between Chamber_Af and extrapolated Chamber_Bf must be significant. We use T-test and 95% confidence interval.

Criterion 2: The slope of all data points or the first 8 data points during the Chamber_Af period is significantly different from the slope of aerosol concentration during the Chamber_Bf period. The rationale behind this criterion is that if the perturbation causes a substantial change in the concentration of an OA factor, its slope during the Chamber_Af period should be different from that during the Chamber_Bf period.

The slope of aerosol concentration during the Chamber_Af period is obtained in the following way. We calculate the slope by using (1) all data points and (2) only first 8 data points during the Chamber_Af period. This is because the concentration of factors firstly increases after perturbation and then decreases due to dilution (Fig. A1). In this case, the slope obtained by fitting all data points might be negative and will not reflect the initial increase in concentration (e.g., LO-OOA of ap_0805_1 in Fig. S4a). Using only the first few data points during the Chamber_Af period can avoid this issue. We select the first 8 data points in this period because the concentrations of total OA and OA factors typically reach the highest at the 8th point (i.e., ~16min after injection). The slope is calculated by Theil-Sen estimator.

The slope of aerosol concentration during the Chamber_Bf period is analyzed in the following way. In order to determine if the slope in Chamber_Af is significantly different from that in Chamber_Bf, we use bootstrap analysis (1000 times) to obtain a distribution of the slope of Chamber_Bf. In brief, in each random resampling of Chamber_Bf with replacement, a slope is calculated by Theil-Sen estimator. Then, 1000 times resampling provides a distribution of slope in Chamber_Bf. The 5% and 95% percentiles of the slope distribution are compared to the slope of Chamber_Af to determine if the slopes are significantly different. If the slope of Chamber_Af (from either all data points or the first 8 data points) is smaller (or larger) than the 5% (or 95%) percentile, the slopes in Chamber_Bf and Chamber_Af are significantly different.

Criterion 3: The slope of all data points or the first 8 data points during the Chamber_Af period is significantly different from the slope of ambient data (i.e., combined Amb_Bf and Amb_Af). The rationale behind this criterion is the same as the second criterion. That is, if the perturbation causes a substantial change in the concentration of an OA factor, its slope during the Chamber_Af period should be different from that in ambient data. The procedure to obtain a distribution of slopes in the ambient data (combined Amb_Bf and Amb_Af) is same as Criterion 2.

As mentioned above, one critical assumption is that the ambient variation is linear during both the Chamber_Bf and Chamber_Af periods (i.e., when instruments are connected to chamber and not sampling the ambient aerosol) and that the ambient variation can be represented by interpolating Amb_Bf and Amb_Af. We design the following pseudo-experiment to test the validity of this assumption. In brief, we perform the same analysis as we did for the perturbation experiments, but using ambient data **only** (i.e., no perturbation data). We firstly randomly select a data point, which defines the start point of one pseudo-test. Secondly, based on the start point, we obtain the concentration of OA factors during "Amb_Bf" period, (i.e., from start point to start point + 30min), "Chamber_Bf" period (i.e., from start point + 30min to start point + 60min), "Chamber_Af" period (i.e., from start point + 60min to start point + 100min), and "Amb_Af" period (from start point + 100 min to start point + 130min). This mimics the sampling periods in a real perturbation experiment. Thirdly, we calculate the slope of ambient period (i.e., combined "Amb_Bf" and "Amb_Af" periods) and the slope of chamber period (i.e., combined "Chamber_Bf" and "Chamber_Af" periods). Fourthly, we calculate if the slope of chamber period is significantly different from the slope of ambient period. We repeat this test 1000 times and then obtain the probability of whether the slopes of chamber period and ambient period are significantly different.

Fig. A2a shows the probability that the slopes of chamber period and ambient period are not significantly different for five factors. The larger this probability is, the more reliable the linearity assumption is. The average probability is ~50% for all factors, without discernible diurnal trends. This suggest that there is ~50% chance that the linear variation assumption is valid. Since the linearity assumption is not perfect, we develop another criterion to constrain the potential influence of ambient variation on the interpretation of perturbation results.

Criterion 4: From the above pseudo-experiment on ambient data only, we can calculate the relative change in slope between "chamber period" and "ambient period" by

$$\text{relative change in slope} = \frac{\text{Slope}_{\text{Chamber}} - \text{Slope}_{\text{Amb}}}{\text{Slope}_{\text{Amb}}} \quad \text{Eqn 1}$$

In each pseudo-experiment test, we calculate a relative change in slope between "chamber period" and "ambient period". By repeating the pseudo-experiment test 1000 times, we obtain a frequency distribution of the relative change in slope for each OA factor (Fig. A2b). This frequency distribution indicates the probability that certain relative change in slope occurs due to ambient variation. Take LO-OOA as an example, the probability that the relative change in slope varies by

a factor 8 due to ambient variation is ~1%. Thus, if the relative change in slope of LO-OOA in a α-pinene experiment is 8, the change is unlikely due to ambient variation. We use the 5% and 95% percentiles from the frequency distribution as the fourth criterion to determine if the changes in the concentrations of OA factors in each perturbation experiment are due to ambient variation. In other words, if the relative change in slope between Chamber_Af and ambient data in a real perturbation experiment falls outside of the 5% or 95% percentiles, the changes in the concentrations of OA factors are likely due to perturbing chamber with VOC, instead of ambient variation. This criterion strictly considers the influence of ambient variation. In general, the comparison in slope is an optimal option to account for ambient variation, because the influence of ambient variation is unlikely to coincide with the perturbation.

Based on these 4 criteria, the OA factors with significant changes in their mass concentrations as a result of perturbation are shown in Fig. 4. LO-OOA is enhanced in 14 out of 19 α-pinene experiments. However, total OA is only enhanced in 8 out of 19 α-pinene experiments. Several reasons can contribute to the different behaviors of LO-OOA and OA. Firstly, as total OA has multiple sources, the enhancement in one factor does not guarantee an enhancement of total OA. For instance, in some perturbation experiments, while LO-OOA is enhanced, the concentration of other factors steadily decreases due to ambient variation. The increase in LO-OOA and decrease in other factors compensate each other and result in a lack of enhancement in total OA. Secondly, based on the pseudo-experiment, we note that total OA is more easily affected by ambient variation than a single OA factor. For example, the 95% of the relative change in slope of total OA is 3.59, which is larger than any OA factors (Fig. A2b). Thus, the criteria for the change in total OA concentration to be considered as significant are stricter than those for a single OA factor. Thus, some experiments with significant changes in LO-OOA do not have significant changes in total OA.

Atmos. Chem. Phys. Discuss., https://doi.org/10.5194/acp-2017-1109
Manuscript under review for journal Atmos. Chem. Phys.
Discussion started: 2 January 2018

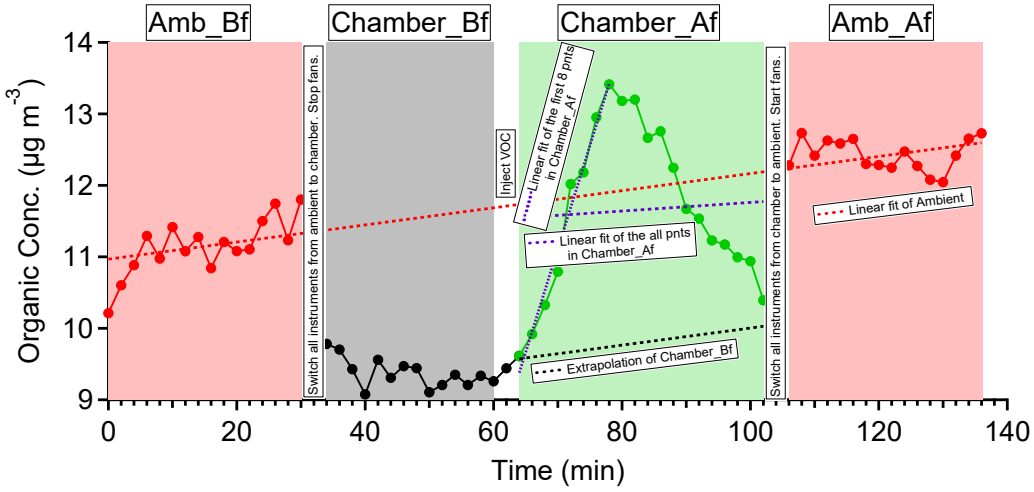

Fig. A1. Time series of OA in experiment ap_0801_1 to illustrate the analysis method. Each perturbation experiment includes four periods: Amb_Bf (~30min), Chamber_Bf (~30min), Chamber_Af (~40min), and Amb_Af (~40min). "Amb" and "Chamber" correspond to the periods when the instruments are sampling ambient and chamber, respectively. "Bf" and "Af" stand for before and after perturbation, respectively. The solid lines are measurement data. The dashed red lines are the linear fit of ambient data (i.e., combined Amb_Bf and Amb_Af). The slope is used to extrapolate Chamber_Bf data to Chamber_Af period (i.e., black dashed line). The dense dashed purple line is the linear fit of the first 8 points during the Chamber_Af period. The sparse dashed purple line is the linear fit of all data points during the Chamber_Af period. During this period, the difference between measurements (i.e., solid green data points) and extrapolated Chamber_Bf (i.e., dashed black line) represents the change in organic concentration caused by perturbation.

Atmos. Chem. Phys. Discuss., https://doi.org/10.5194/acp-2017-1109
Manuscript under review for journal Atmos. Chem. Phys.
Discussion started: 2 January 2018

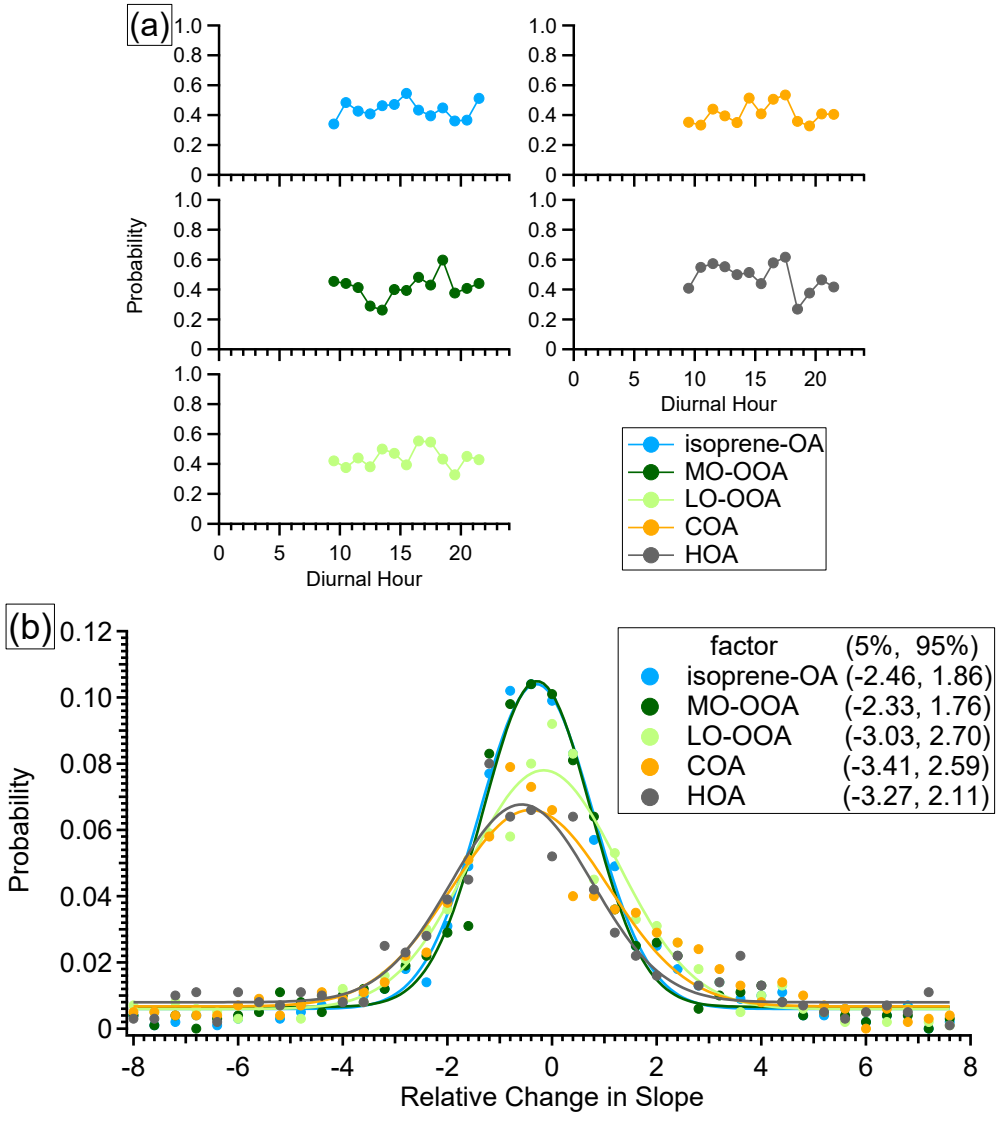

Fig. A2. (a) The diurnal trends of the probability that the slopes between ambient periods (i.e., Amb_Bf and Amb_Af periods) and chamber periods (i.e., Chamber_Bf and Chamber_Af periods) are not significantly different in the pseudo-experiment. (b) The frequency distribution of the relative change in slope. The data points are fitted using Gaussian function. The numbers in the box represent the 5% and 95% percentile of the Gaussian fit.

Atmos. Chem. Phys. Discuss., https://doi.org/10.5194/acp-2017-1109
Manuscript under review for journal Atmos. Chem. Phys.
Discussion started: 2 January 2018

Appendix B. Ambient Perturbation Experiments with Acidic Sulfate Particles

Previous field observations showed strong correlation between isoprene-OA and sulfate (Xu et al., 2015a; Xu et al., 2016; Budisulistiorini et al., 2015). Moreover, airborne measurements over power plant plumes in Georgia, U.S. observed enhanced isoprene-OA formation in the sulfate-rich power plant plume (Xu et al., 2016). To probe the relationship between isoprene-OA and sulfate, we conducted perturbation experiments in August 2015 by injecting acidic sulfate particles (i.e., a mixture of H_2SO_4 and $MgSO_4$) into the 2 m^3 Teflon chamber. This mimics the airborne measurements over power plants, which introduce sulfate into the atmosphere (Xu et al., 2016).

The experimental procedure in 2015 experiments is generally similar to those in 2016 experiments, but has the following modifications. Firstly, in order to avoid the depletion of species which can uptake to sulfate particles, we kept one fan on during the Chamber_Bf and Chamber_Af periods to enhance the air exchange between chamber and atmosphere. Secondly, considering the fan is on during sulfate injection to enhance mixing chamber air with ambient air, we only use the Chamber_Bf and Chamber_Af periods to calculate the changes in OA factors. The Criteria (1)(2)(4) are applied in 2015 experiments. Thirdly, the Chamber_Bf period is ~40 min in 2015 experiments, which is slightly longer than the 30 min in 2016 experiments. Fourthly, the HR-ToF-CIMS was not deployed in 2015 experiments.

The acidic sulfate seed particles were introduced into chamber by atomizing 0.88mM H_2SO_4 + 0.48mM $MgSO_4$ mixture solution from a nebulizer (U-5000AT, Cetac Technologies Inc., Omaha, Nebraska, USA). One important interference in these sulfate perturbation experiments is the trace amount of organics in solvent water [i.e., HPLC-grade ultrapure water (Baker Inc.)], which is used to prepare the H_2SO_4+$MgSO_4$ solution. These organics were injected into chamber together with sulfate. We utilize the multilinear engine solver (ME-2) to constrain the organics from solvent water (i.e., H_2O-Org). Unlike the PMF2 solver which does not require any a priori information of mass spectrum or time series, the ME-2 solver uses a priori information to reduce rotational ambiguity among possible solutions(Canonaco et al., 2013; Paatero, 1999). We obtained the reference spectrum of organic contamination (i.e., the a priori information for ME-2 solver) by atomizing the H_2SO_4+$MgSO_4$ solution directly into AMS. The ME-2 solver successfully extracted a factor (i.e., denoted as H_2O-Org factor, Fig. B1), which showed a clear enhanced concentration during atomization (Fig. B2).

A total of four experiments were performed and details are summarized in Table B1. As shown in Fig. B2, the isoprene-OA factor increases in all three daytime experiments, but not the nighttime experiment. Based on current understanding of isoprene-OA factor, this enhancement is likely due to the reactive uptake of IEPOX. The lack of enhancement in nighttime experiment is consistent with low IEPOX concentration at night (Hu et al., 2015). Our results provide direct observational evidence that acidic sulfate particles lead to increase in isoprene-OA, which supports results from previous studies (Xu et al., 2015a; Xu et al., 2016; Budisulistiorini et al., 2015). Due to lack of measurements of gas-phase organic compounds, we are unable to identify the reactive species. Other species, such as glyoxal (Kroll et al., 2005), isoprene hydroperoxides (Liu et al., 2016), and HOMs (Ehn et al., 2014), also have the potential to uptake to acidic sulfate particles and form SOA. Future experiments with comprehensive measurements of gas-phase organic compounds can provide more insights into the identities of reactive uptake species.

We note that in non-atomizing period, the concentration of H_2O-Org factor is close to zero, but not zero. Since H_2O-Org arises from the atomizing solution, it should only exist during atomizing periods. Thus, the non-zero concentration suggests the limitation of the ME-2 solver and cautions are required when using ME-2 solver to resolve one factor based on a specific mass spectrum. This limitation does not affect the conclusion that the enhancement in isoprene-OA is likely due to the reactive uptake of organic species, as we further verify that the organic increase in three daytime perturbation experiments with sulfate particles cannot be solely explained by the organic contamination in atomizing water, from the following two aspects. For example, we atomize the solution directly into AMS and find that the Org/SO_4 ratio is 0.025. This value is significantly lower than the Org/SO_4 ratio in the three daytime sulfate perturbation experiments (i.e., 0.048-0.059), but close to the nighttime sulfate perturbation experiment (i.e., 0.022) (Fig. B4).

Atmos. Chem. Phys. Discuss., https://doi.org/10.5194/acp-2017-1109
Manuscript under review for journal Atmos. Chem. Phys.
Discussion started: 2 January 2018

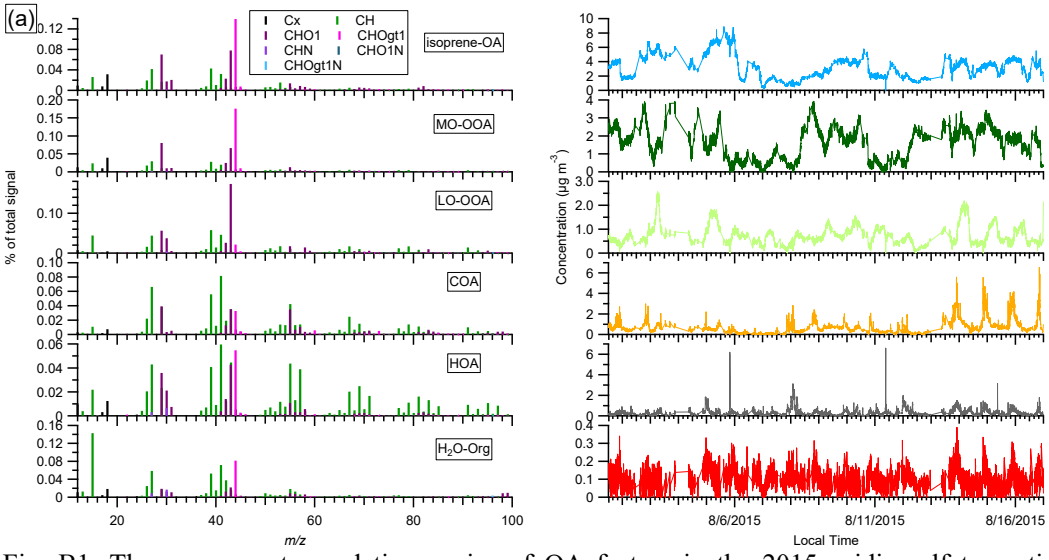

Fig. B1. The mass spectra and time series of OA factors in the 2015 acidic sulfate particle perturbation measurements. Note that the perturbation periods are included in the time series.

Atmos. Chem. Phys. Discuss., https://doi.org/10.5194/acp-2017-1109
Manuscript under review for journal Atmos. Chem. Phys.
Discussion started: 2 January 2018

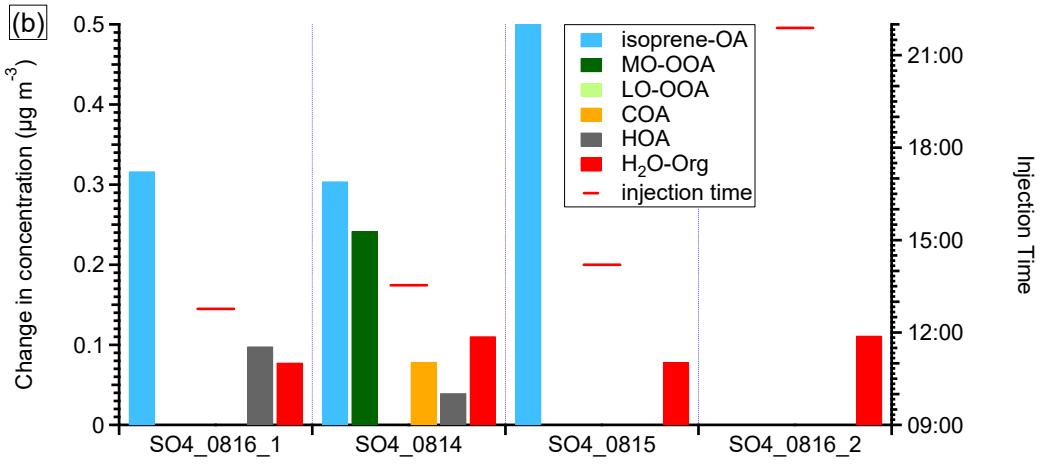

Fig. B2. The statistically significant changes in the concentrations of OA factors after perturbation by acidic sulfate particles. The experiments are sorted by perturbation time. The changes in concentration are the difference between measurements during the Chamber_Af period and mass concentration extrapolated from the Chamber_Bf period. A set of criteria are developed to evaluate if the changes are significant and if the changes are due to ambient variation (Appendix A). H_2O-Org factor in these sulfate perturbation experiments represents organic contaminations in atomizing water.

Atmos. Chem. Phys. Discuss., https://doi.org/10.5194/acp-2017-1109
Manuscript under review for journal Atmos. Chem. Phys.
Discussion started: 2 January 2018

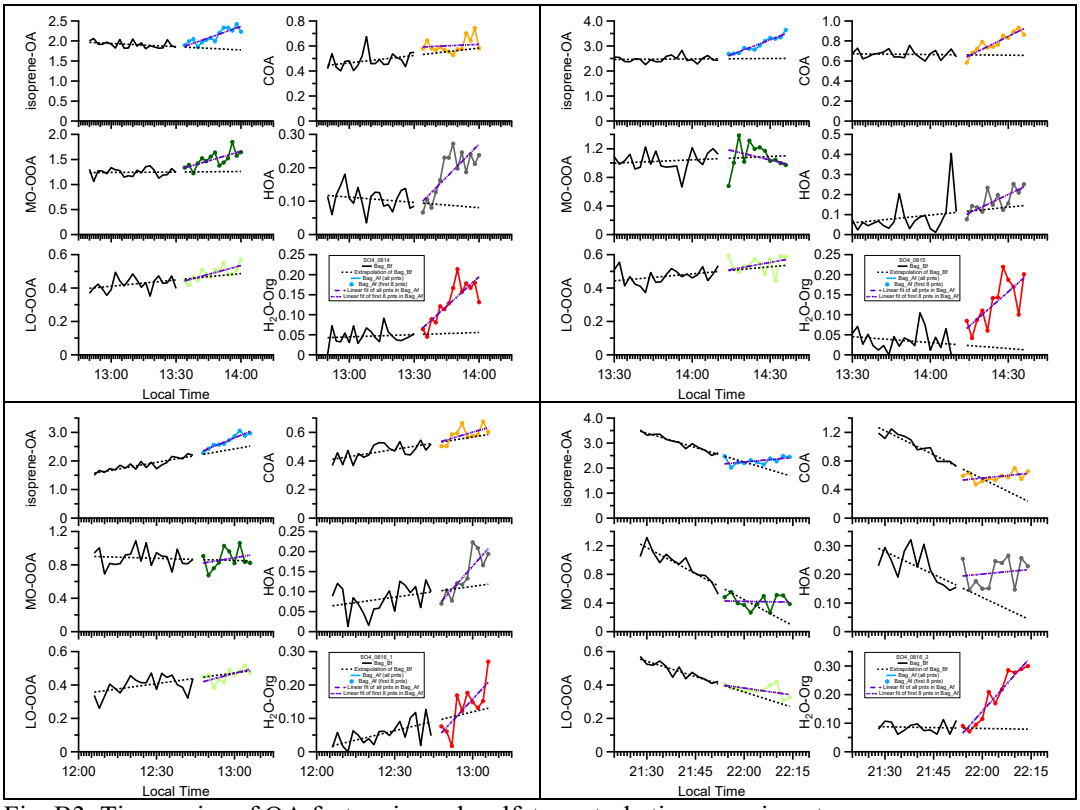

Fig. B3. Time series of OA factors in each sulfate perturbation experiment.

Atmos. Chem. Phys. Discuss., https://doi.org/10.5194/acp-2017-1109
Manuscript under review for journal Atmos. Chem. Phys.
Discussion started: 2 January 2018

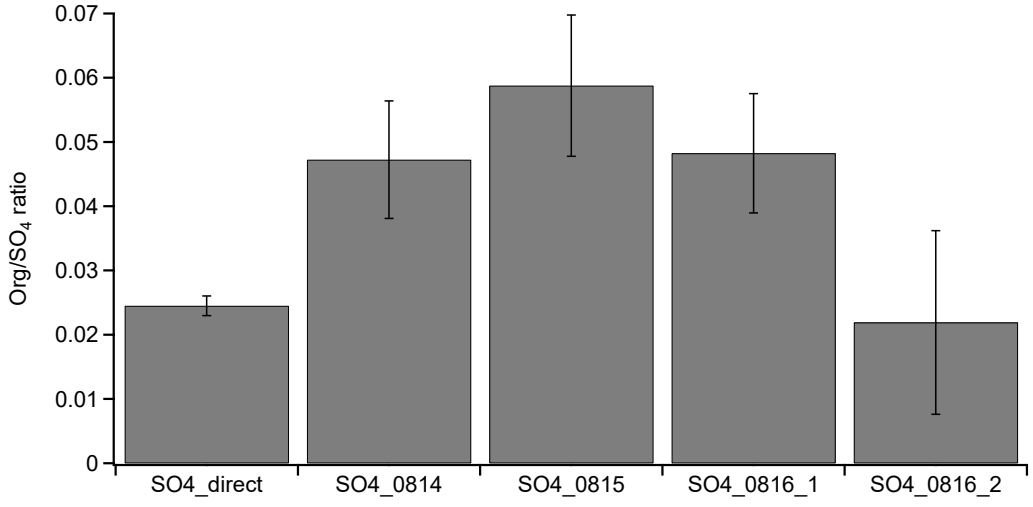

Fig. B4. The Org/SO_4 ratio in sulfate perturbation experiments and laboratory tests by directly atomizing H_2SO_4 + $MgSO_4$ mixture solution into AMS (i.e., SO4_direct).

Atmos. Chem. Phys. Discuss., https://doi.org/10.5194/acp-2017-1109
Manuscript under review for journal Atmos. Chem. Phys.
Discussion started: 2 January 2018

Atmospheric Chemistry and Physics Discussions

Table B1. Experimental conditions for sulfate perturbation experiments.

Perturbation	Expt ID[a]	Date	Injection Time	Perturbation Amount[b]	NO[c] (ppb)	NO_2[c] (ppb)	O_3[c] (ppb)
sulfate	SO4_0814	8/14/2015	13:32	16.29	0.51	5.86	59.8
	SO4_0815	8/15/2015	14:12	14.33	0.18	4.79	63.0
	SO4_0816_1	8/16/2015	12:46	14.52	0.36	4.08	53.2
	SO4_0816_2	8/16/2015	21:53	13.92	0.03	5.40	35.6

[a]Expt ID is named as "perturbation species + date + experiment number". For example, SO4_0816_1 represents the first sulfate perturbation experiment on 08/16.

[b]The unit for the perturbation in sulfate experiments is $\mu g\ m^{-3}$. The perturbation amounts of sulfate are calculated from Chamber_Af – extrapolated Chamber_bf.

[c]Average concentration during the Chamber_Af period.